8-2006

Changes in Microbial Community Structure of Petroleum Contaminated Sediments are Reflected in Subsurface Geophysical Signatures

Jonathan P. Allen

CHANGES IN MICROBIAL COMMUNITY STRUCTURE OF PETROLEUM CONTAMINATED SEDIMENTS ARE REFLECTED IN SUBSURFACE GEOPHYSICAL SIGNATURES

by

Jonathan P. Allen

A Thesis
Submitted to the
Faculty of The Graduate College
in partial fulfillment of the
requirements for the
Degree of Master of Science
Department of Biological Sciences

Western Michigan University
Kalamazoo, Michigan
August 2006

ACKNOWLEDGMENTS

I would like to acknowledge those people who have helped me throughout this entire process. First and foremost, I would like to thank my advisor Dr. Silvia Rossbach for her invaluable guidance and support. I would also like to recognize my committee members, Dr. Estella Atekwana, Dr. Todd Barkman, and Dr. Steven Kohler. Their critical review of my work has been extremely helpful in the completion of this thesis.

I would also like to recognize Dr. Eliot Atekwana for his work on the geochemical analysis within the field and laboratory, construction of the laboratory columns, and review of this manuscript, Dr. D. Dale Werkema for his design and installation of the vertical resistivity probes and geophysical measurements in both the field and laboratory, and Joe Duris for collection of the field sediment samples and early microbial work with the laboratory columns.

Finally, I would like to thank Evelyn Sirisani and Sceone Sloan for their help with the 16S rRNA gene libraries, especially the countless number of plasmid purifications.

Jonathan P. Allen

CHANGES IN MICROBIAL COMMUNITY STRUCTURE OF PETROLEUM CONTAMINATED SEDIMENTS ARE REFLECTED IN SUBSURFACE GEOPHYSICAL SIGNATURES

Jonathan P. Allen, M.S.

Western Michigan University, 2006

Petroleum contamination of sediments leads to dynamic changes in the subsurface. These include changes in the microbiota as well as in the subsurface geophysical and geochemical properties. Anomalously high conductivity values observed in subsurface zones contaminated with light non aqueous phase liquids (LNAPLs) have been suggested to be the result of microbial activity. Therefore, we investigated the interdependence between geoelectrical signatures and microbial community structure in petroleum contaminated field sediments and laboratory column experiments. Spatial and temporal changes in electrical conductivity of the subsurface paralleled changes in microbial community composition, with the highest conductivity values concomitant with specific anaerobic hydrocarbon-degrading populations. We surmise that with an abundant carbon source such as petroleum hydrocarbons, increased microbial activity results in the physical and chemical alteration of the immediate environment, effectively changing the subsurface geophysical properties within those zones. We suggest that geoelectrical measurements are an efficient tool to guide sampling for microbial ecology studies during the monitoring of natural or engineered bioremediation projects.

TABLE OF CONTENTS

Table of Contents—continued

LIST OF TABLES

LIST OF FIGURES

CHAPTER I

INTRODUCTION

Widespread petroleum contamination of the subsurface from surface spills and damaged underground storage tanks (UST) remains a significant environmental problem. The United States Environmental Protection Agency (EPA) reports a backlog of over 150,000 cases of leaking UST yet to be addressed (U.S.EPA, 2006). Traditional physical and chemical removal of contaminant compounds is difficult, and exposes workers to dangerous pollutants (Atlas, 1995). Alternative natural attenuation strategies provide an efficient approach for contaminant removal (Tulis, 1997). It is well established that the microbial degradation of hydrocarbons leads to effective reduction of the hydrocarbon contaminant mass in natural settings (Kaplan & Kitts, 2004; Macnaughton *et al.*, 1999; Margesin & Schinner, 2001; Roling *et al.*, 2004; Van Hamme *et al.*, 2003; Venosa *et al.*, 1996; Whiteley & Bailey, 2000) However, the monitoring of microbial activity and contaminant degradation can be very costly and time consuming.

The subsurface contaminated by petroleum hydrocarbons, especially with light non aqueous phase liquids (LNAPLs), represents a complex environment (Sauck, 2000). In subsurface sediments, the LNAPLs partition into dissolved, free, and residual phases. The dissolved phase is represented by hydrocarbons dissolved in groundwater, while the free phase contamination consists of pure hydrocarbons floating on top of the groundwater table. The residual phase LNAPLs occur above and

below the free phase where hydrocarbons adhere to the sediments in a smear zone due to the fluctuations of the groundwater table (Lee *et al.*, 2001). In addition to this vertical stratification, variations occur in the LNAPL distribution due to contaminant transport, and the physical, chemical, and biological attenuation of the LNAPLs, which contribute to the subsurface complexity of contaminated sediments.

The growth of microorganisms and their metabolic activities in petroleum contaminated sites alter the physical and chemical conditions of their environment. Physical alterations result from colonization of sediment surfaces and reduction of pore space between sediments by microbial growth in the form of biofilms (Banfield *et al.*, 2000). Chemical alterations can occur via reduction of the contaminant mass resulting in the production of metabolic byproducts such as organic acids and CO_2. The organic and carbonic acids formed during the microbial biodegradation of hydrocarbons invariably release ions from the sediment grains (weathering) or remove ions from the pore water (precipitation). The degree to which microorganisms alter the physical and chemical conditions within the contaminated environment depends on a range of variables including the microbial community structure, microbial physiology, and the environmental and geological conditions (Haack & Bekins, 2000; Walworth & Reynolds, 1995; Zhou *et al.*, 2004). The change imparted to the geologic environment by microbial hydrocarbon biodegradation alters the physical properties of the subsurface in such a way that can be detected using geophysical techniques.

Geophysics analyzes the physical properties in the outer surface of the Earth in order to determine the nature, composition, and contour of the subsurface. Geophysical methods involving seismology and ground penetrating radar have been successfully used in mapping the subsurface for water saturation, sediment lithology,

and subsurface contamination (Telford *et al.*, 1990). Recently, geophysical methods investigating the electrical conductivity of aged petroleum contaminated sediments have shown anomalously high conductivity values within the hydrocarbon contaminant zone at spill sites at a former Air Force Base in Oscoda, MI and at a former refinery site in Carson City, MI (Atekwana *et al.*, 2000; Atekwana *et al.*, 2004a; Bermejo *et al.*, 1997). Petroleum hydrocarbons naturally have insulating properties, and when introduced into the subsurface, they fill the pore spaces creating an electrically resistive contaminant zone above the water table (DeRyck *et al.*, 1993). Therefore the high conductivity of these sediments at petroleum spill sites was unexpected.

Previous field work at the Carson City site completed by Duris (2002) investigated the impact of microbial activity on geophysical properties of the petroleum contaminated sediments by studying the microbial populations present in zones of higher and lower electrical conductivity. Using a culture-dependent most probable number (MPN) method, it was shown that an increase in the proportion of hydrocarbon degrading microorganisms was concomitant with the level of LNAPL saturation, and increased electrical conductivity (Duris, 2002). However, because only a small percentage of microorganisms can be cultured in the laboratory, culture-independent ribosomal intergenic spacer analysis (RISA) was used in addition to the MPN method in order to provide further information into the microbial community changes which existed in zones of different LNAPL contamination and electrical conductivity. The results of the RISA profiles demonstrated that changes in the microbial community paralleled changes in the electrical conductivity and petroleum contamination over a vertical gradient in the subsurface (Duris, 2002). These results demonstrated a possible relationship between the activities of microbial communities

in petroleum contaminated sediments and subsurface geophysical properties. However, no studies have been performed which characterize the microbial community structure to identify specific microbial populations or processes within these conductive zones which may be involved in altering the subsurface geophysical properties of petroleum contaminated sediments.

The above investigations provide evidence for complex biogeophysical relationships in the contaminated subsurface, and demonstrate the need for further detailed studies evaluating how microbial activities and microbial growth can result in anomalous geoelectrical subsurface properties. Our hypothesis is that the changes in the microbial community structure of petroleum contaminated sediments are reflected in the subsurface geophysical properties. Analysis of the microbial community structure can be used to evaluate the connections between microbially driven processes and the induced environmental changes measured by geophysical techniques (Newman & Banfield, 2002). In this study we investigated the biogeophysical relationships of petroleum contaminated sediments in two main experimental designs. In the first part we utilized culture-independent 16S rRNA gene sequencing coupled with electrical conductivity measurements at a petroleum contaminated field site. The goals were to: (1) characterize microbial community composition in zones of increased electrical conductance, (2) determine if spatial changes in the microbial community structure could explain the observed geoelectrical measurements, and (3) identify microbial populations and processes which may be involved in the enhancement of the sediment's electrical conductivity. In the second part of this study we constructed laboratory scale mesocolumns to simulate petroleum contaminated and background conditions in order to monitor changes in microbial community structure in relation to changing subsurface

geophysical properties. We analyzed the microbial community using a culture-based MPN analysis to determine the amount of hydrocarbon degrading microorganisms, as well as culture-independent RISA to observe overall changes in the community structure, and 16S rRNA gene sequencing to determine which microbial populations have the greatest impact on subsurface geophysical properties in petroleum contaminated sediments. The results of this study suggest a link between the geophysical properties of hydrocarbon contaminated sediments and microbial community structure, and reveal the complex biogeophysical relationships which exist in petroleum contaminated sediments.

CHAPTER II

MATERIALS AND METHODS

Site Description

The study site is a city park containing an underground petroleum hydrocarbon plume adjacent to the former Crystal Refinery Company in Carson City, Michigan, USA (Fig. 1). Continuous release of hydrocarbons (mainly crude oil, JP4 jet fuel, and diesel fuel) occurred from underground storage facilities for over 50 years. The aquifer is about 2 m thick and composed of loam soils and glacio-fluvial sands and gravels underlain by clay. The mineralogy of the aquifer is predominantly quartz with minor calcite, albite, anorthite, gypsum, and dolomite (Dell-Engineering, 1992).

The contaminated portion of the aquifer has hydrocarbons in the dissolved, free and residual phase. The free-phase petroleum zone is up to 0.6 m thick above the water table. The residual phase contaminated zone averages about 1 m above and below the free product contaminated zone due to annual fluctuation of the groundwater table of 0.9 m (Dell-Engineering, 1992). In this study, we collected geophysical data and sediments for microbial analyses from a contaminated location with residual, free, and dissolved phase LNAPL (VRP5) and an uncontaminated background location (VRP9) in August of 2000.

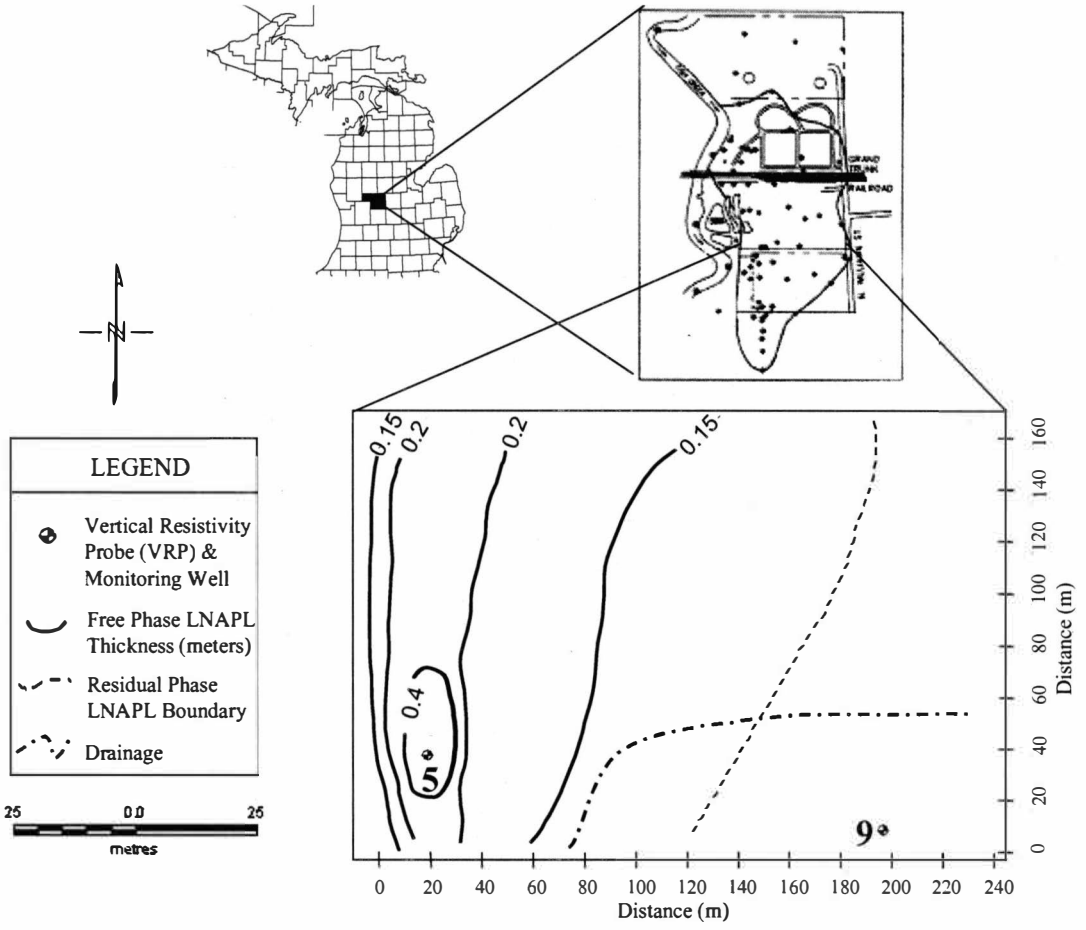

Figure 1. Detailed Map of the Field Study Site Within the Carson City Park, Carson City, MI. The instrument positions (Vertical Resistivity Probes, VRP) are noted for the contaminated (VRP5) and background (VRP9) locations. Samples for microbial analysis were collected at the same locations, adjacent to the VRPs. To the north of the sample site is the old petroleum refinery where the leaking underground storage tanks were located. The contaminant plume flows from the source toward the adjacent Fish Creek to the west. The free phase LNAPL thickness is given over the study area (solid lines), as well as the boundary of residual LNAPL contamination (dashed line). The location of a drainage ditch running through the site is shown (dash-dotted line).

Laboratory Column Construction

The experimental columns were constructed out of 80 cm long by 31 cm diameter polyvinyl chloride pipe (PVC) (Fig. 2). The columns were filled with autoclaved fine to medium-grained sands composed of quartz with minor quantities of feldspars and carbonates obtained from sediments adjacent to a contaminated site in Carson City, Michigan (Werkema, 2002). Five pre-fabricated sediment cores to be used for microbial analysis were placed in the columns prior to filling with sand. The cores were made of 2.5 cm diameter PVC pipe cut in half lengthwise and wrapped in mesh covering so the sediments within the core were open to the environment. The bacterial inoculum used in the columns was obtained by shaking sands collected within the upper residual LNAPL zones from the Carson City site in a 25% Bushnell-Haas (BH) medium (Becton Dickinson, Detroit, MI) in a 1:10 ratio (Duris, 2002).

The columns were constructed to simulate typical field sediments with the ground water table set at a 45 cm depth. The control column, representing background field conditions, contained a diluted nutrient solution of 25% BH medium, along with the bacterial inoculum. The contaminated column was additionally amended with 4 L of diesel fuel. Contamination was accomplished by filling the column with 25% BH medium, followed by addition of the diesel fuel at the top of the column, and finally draining the BH medium down to the 45 cm ground water table depth. This resulted in diesel smear (residual phase) on the sediment grains from 0 to 32 cm, sediments with free phase diesel from 32 to 45 cm, and dissolved phase diesel contamination in the water saturated zone below 45 cm. During construction the control column was also filled with 25% BH medium and drained to 45 cm depth, but no diesel was added. The columns were maintained at room temperature.

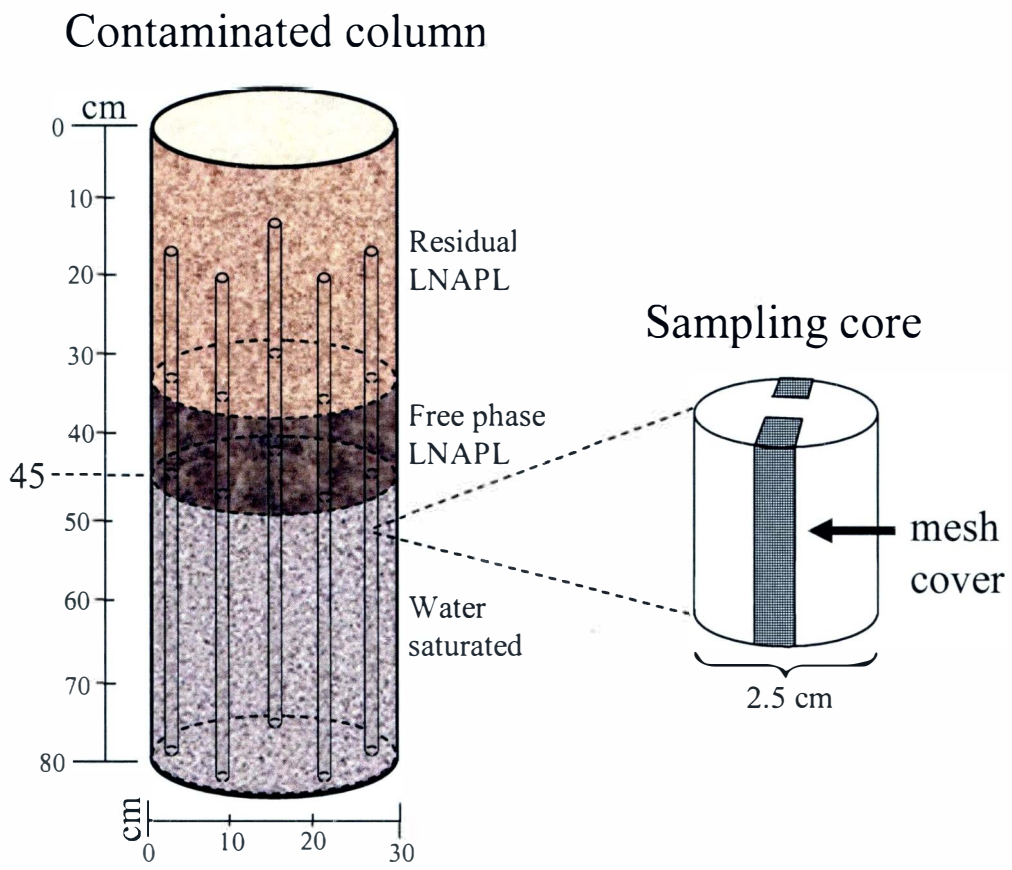

Figure 2. Laboratory Column Setup. In both columns the water table was located at a 45 cm depth. In the contaminated column (shown here), the LNAPL contamination existed as residual contamination in the upper sediments, as free phase LNAPL floating above the water table, and as dissolved LNAPL in the water saturated zone. Five cores used for microbial sampling are shown within the column. The subset of the sample core shows the mesh siding of the core for free interaction with the surrounding environment.

Sediment Sampling, Cell Extraction, and DNA Purification

Sediment samples from the field site were collected by coring adjacent to the VRPs. Samples were collected in sanitized core liners fitted into a hand operated direct push soil coring device. After coring, the liners were removed and immediately

capped, secured with electrical tape, and transported to the laboratory on ice. Sediment samples from the laboratory columns were collected by removal of the sampling cores installed during column construction. Sediment subsamples used for culture-dependent analysis were weighed and approximately 1 g of soil was placed into sterilized 15 ml polypropylene tubes for cell extraction. The tubes were filled with 9.5 ml of 0.1% sodium pyrophosphate and shaken at 250 rpm for 30 min to remove cells. Tubes were then centrifuged at 900g for 10 minutes, and the supernatant was collected and used immediately for Most Probable Number (MPN) analysis. For molecular analysis, an aliquot of soil was stored at -20°C. Total chromosomal DNA was purified from sediment subsamples using the MoBio Ultra Clean Soil DNA Kit (MoBio, Solana Beach, CA) per manufacturer instructions, and stored at -20°C.

Most Probable Number (MPN) Analysis

For bacterial enumerations, 25 µl aliquots of extracted cells were inoculated into the first well of four rows in 96 well microtiter plates. The microtiter plates contained 225 µl of BH medium (Becton Dickinson, Detroit, MI) supplemented with 6.25 µl (2.5%) of n-hexadecane for estimation of the hydrocarbon degrading population. Serial dilutions were performed to a final 10-10 dilution, and incubated at room temperature for two weeks. For evaluation of microbial growth in the BH plates, 50 µl of p-iodonitrotetrazolium violet (3 g/l) was added to each well, and incubated for an additional 24 hrs at room temperature. Plates were visually examined for an appearance of a red precipitate indicating positive growth, and scored accordingly (Wrenn & Venosa, 1996). Once the plates were scored, the results were entered into the Most Probable Number Calculator version 4.04 to determine the most probable

number of bacteria per gram of soil as compared to published MPN charts (Klee, 1993).

Ribosomal Intergenic Spacer Analysis (RISA)

The intergenic spacer region between the 16S and 23S rRNA genes was amplified from total chromosomal DNA by polymerase chain reaction (PCR). The region was amplified in 50 µl reaction mixtures containing (as final concentrations) 50 mM KCl, 1.5 mM MgCl2, 10 mM Tris-HCl (pH 8.3), 0.01% gelatin, a 0.2 mM concentration of each deoxyribonucleotide, 100 pmol of each forward and reverse primer, and 1U of Red-Taq DNA polymerase (Sigma-Aldrich Corp, St. Louis, MO). PCR was carried out in an Eppendorf MasterCylcer Gradient DNA Thermal Cycler (Eppendorf, Westbury, NY) with an initial denaturing step for 2 min at 94°C followed by 32 cycles at 94°C for 1 min, 55°C for 2 min, and 72°C elongation for 3 min, followed by a final elongation at 72°C for 5 min. The primers used were 1406F (5'-TGYACACACCGCCCGT-3') (universal for 16S rRNA gene) and 23SR (5'-GGGTTBCCCCATTCRG-3') (bacterial 23S rRNA gene) (Borneman & Triplett, 1997). PCR products were run on a 1.2% agarose gel with Tris-Borate-EDTA (TBE) buffer for 24 hrs at 4°C, and visualized by ethidium bromide staining under ultraviolet light.

Construction of 16S Ribosomal RNA Gene Libraries

Community 16S rRNA genes were PCR amplified from the bulk DNA in 50 µl reaction mixtures containing (as final concentrations) 50 mM KCl, 1.5 mM MgCl2, 10 mM Tris-HCl (pH 8.3), 0.01% gelatin, a 0.2 mM concentration of each deoxyribonucleotide, 100 pmol of each forward and reverse primer, and 1.5 U of Red-

Taq DNA polymerase (Sigma-Aldrich Corp, St. Louis, MO). PCR amplifications were carried out in an Eppendorf MasterCycler Gradient DNA Thermal Cycler (Eppendorf, Westbury, NY) with an initial denaturing step for 2 min at 94°C followed by 25 cycles at 94°C for 1 min, 55°C for 1 min, and 72°C elongation for 2 min, followed by a final elongation at 74°C for 7 min. The 16S ribosomal genes from the samples were amplified using the universal oligonucleotide forward primer 8f (5'-AGAGTTTGATCCTGGCTCAG-3') and the universal reverse primer 1492r (5'-CCGTCAATTCMTTTRAGTTT-3') (Hayes & Lovely, 2002), which bind at *E.coli* positions 8 and 907 (Buchholz-Cleven *et al.*, 1997). PCR products were visualized on a 1.2% agarose gel, and purified with a Wizard SV PCR clean-up kit (Promega, Madison, WI). The purified PCR products were cloned with the TOPO TA Cloning Kit, version R (Invitrogen, Carlsbad, CA) in accordance with the manufacturer's instructions. Plasmid DNAs containing inserts were purified from transformed clones using the Eppendorf Fast Plasmid Mini kit (Eppendorf, Westbury, NY) and stored at -20°C for sequencing.

Library Screening, DNA Sequencing, and Phylogenetic Analysis

16S rRNA gene inserts within the plasmid purified from recombinant clones were reamplified by PCR in 50 µl reaction mixtures as stated above. PCR amplification was carried out in an Eppendorf Mastercycler gradient DNA thermal cycler (Eppendorf, Westbury, NY) with an initial denaturing step for 2 min at 94°C followed by 33 cycles of 94°C for 1 min, 55°C for 1 min, and 72°C elongation for 2 min, followed by a final elongation at 74°C for 7 min. The 16S ribosomal gene inserts were amplified using vector primers M13r (5'-CAGGAAAAGCTATGAC-3') and T7f (5'-TAATACGACTCACTATAGGG-3'). Aliquots (7 µl) of the PCR products

were digested with 3 U of restriction endonuclease *Msp*I in 1X NEB buffer 2 (New England Biolabs, Beverly, MA) in a final volume of 10 µl for 1 hr at 37 °C. Digested fragments were separated by agarose (1.2%) gel electrophoresis and visualized by ethidium bromide staining under ultraviolet light. Plasmid inserts from representative clones were sequenced at the Cornell University's Biotechnology Resource Center (Cornell University, Ithaca, NY) using the vector primer M13r. Chimeric sequences were identified by use of the CHECK_CHIMERA program (Cole *et al.*, 2005). The 16S ribosomal gene sequences were compared to the GenBank databases using BLAST (Basic Local Alignment Search Tool) (Altschul *et al.*, 1990), and to the Ribosomal Database Project (RDP) (Cole *et al.*, 2005) to determine their approximate phylogenetic affiliations. Sequence alignments for phylogenetic inference were performed with the CLUSTAL X multiple sequence alignment program (Thompson *et al.*, 1997), and exported for phylogenetic tree construction using PAUP 4.0b (Sinauer Associates, Sunderland, MA). Branching order was determined and compared using distance based neighbor-joining algorithms with Kimura two-parameter correction.

Estimation of Microbial Diversity

The Shannon-Weiner index (H) was calculated using the equation $H' = (-) \sum[P_i(\ln P_i)]$, where P_i is the proportion of individuals found in the ith ribotype of the community (Atlas & Bartha, 1998). Individuals were determined based on *Msp*I RFLP patterns. Equitability (J) was calculated from Shannon-Weiner indices ($J = H'/H_{max}$), where H_{max} is the theoretical maximal Shannon-Weiner diversity index for the population examined ($H_{max} = \ln s$, where s is the total number of different organisms present in the community). The LIBSHUFF program was used to

determine the significance of differences between the 16S rRNA gene libraries (Singleton *et al.*, 2001). Libraries were considered significantly different if the p values were < 0.05.

CHAPTER III

FIELD STUDY

Results

Geoelectrical Measurements

The vertical distribution of the petroleum contaminant in the subsurface of the contaminated location VRP5 is shown in Figure 3A, while the electrical conductivity of the sediments from the contaminated location at VRP5 is shown in Figure 3B. Determination of hydrocarbon distribution in the subsurface was done by Atekwana *et al.*, (2005), and vertical resistivity probe construction and conductivity measurements were done by Werkema (2002). Conductivity values were low (<1 mS/m) from the surface down to the elevation of 225.7 m, where the residual petroleum contamination began. Within the residual contaminated zone to the upper boundary of the free-phase petroleum contaminated zone (225.2 m), the bulk conductivity steadily increased to 15 mS/m. In the free phase petroleum contaminated zone, peak conductivity values were observed between 224.8 m and 225 m elevations, where the conductivity reached up to 49 mS/m. In the water saturated zone with dissolved LNAPL contamination, from 224.8 m to 223.5 m, the conductivity was steadily fluctuating between 13 to 25 mS/m. In fact, below 224.4 m total petroleum hydrocarbon concentrations in the groundwater decreased to undetectable levels (Atekwana *et al.*, 2005).

No petroleum was detected in the background location at VRP9 (Fig. 4A)

(Atekwana *et al.*, 2005). The conductivity measurements for sediments at the uncontaminated location show steadily increasing values up to 7 mS/m from the surface to an elevation of 226.3 m, before decreasing to < 2 mS/m towards the water table (225.3 m) (Fig. 4B). In saturated sediments below the water table, the bulk conductivity increased to steady values of approximately 19 mS/m due to the fluid saturation of the background sediments.

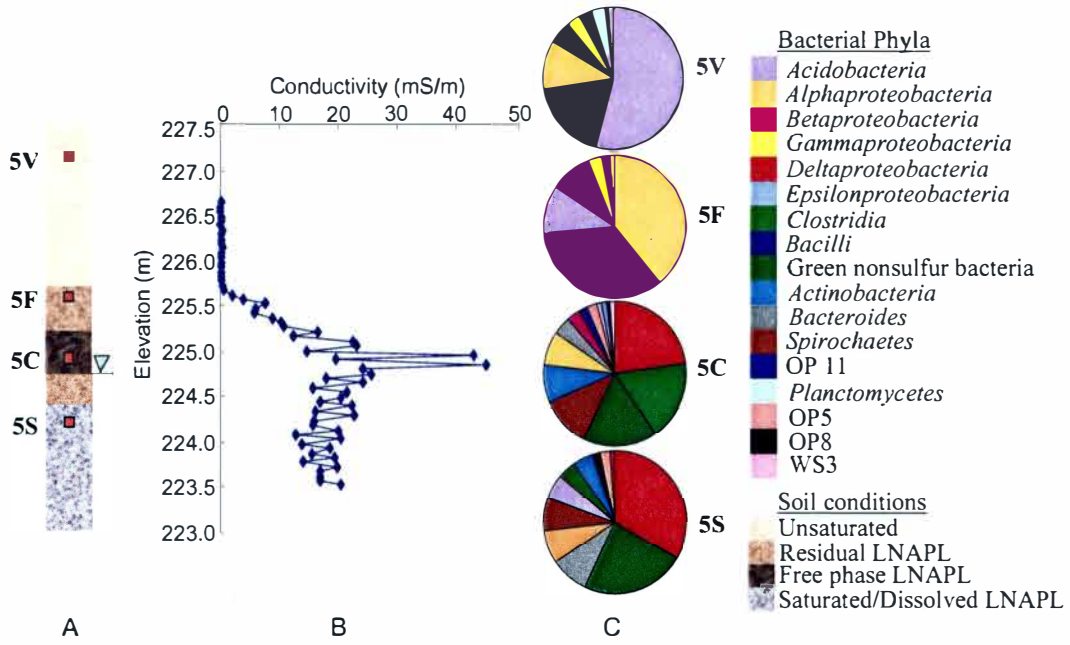

Figure 3. Soil Conditions, Conductivity Profile, and Microbial Community Composition of the Contaminated Site (VRP5). The bar diagram (A) shows the residual and free LNAPL phases, and (B) the vertical sediment conductivity profile is shown. Pie charts (C) show the microbial community composition for sediments from the vadose zone (5V), residual LNAPL contamination in the upper fringe zone (5F), free phase LNAPL contaminant zone (5C), and dissolved LNAPL in the water saturated sediments (5S). The triangle symbol denotes the level of the ground water table, and the red squares denote the sampling depths for the clone libraries.

16S rRNA Gene Library Analysis

In order to determine the microbial community structure from sediments within zones of higher and lower conductivity, 16S rRNA gene libraries were constructed. For the contaminated site (Fig 3A) and background site (Fig 4A), the red squares reflect the depths at which samples for clone library construction were collected. At the VRP5 contaminated site, library 5V was constructed from DNA purified from sediments collected in the upper vadose zone (226.93 m elevation), which exhibited low conductivity readings. Library 5F was constructed from sediments in the upper fringe region of residual LNAPL contamination (225.85 m elevation), where the conductivity began to steadily increase. Library 5C was constructed from the free-phase petroleum contaminated sediments in which the highest conductivity values were recorded (224.93 m elevation), and library 5S was constructed from sediments in the water saturated zone with dissolved contaminant (224.31 m elevation). At the background VRP9 site, the 16S rRNA gene library 9V was constructed from vadose sediments in the unsaturated zone (225.85 m elevation), and library 9S was constructed from sediments in the groundwater saturated zone (224.93 m elevation) (Fig. 4A). A total of 576 different clones containing partial 16S rRNA gene inserts were obtained from the DNA isolated from the sediments samples (Table 1). The 16S rRNA gene inserts were screened for their restriction fragment length polymorphism (RFLP) patterns using the restriction endonuclease *Msp*I and ranked in order of abundance. Libraries 5C and 5S within the free phase and dissolved contamination zones revealed the highest number of identical clones. Out of the 97 total clones in library 5C, one RFLP pattern was represented 13 times, while out of the 95 clones in library 5S, one group of 17 and one group of 10 clones had identical RFLP patterns. Library 5S also contained the lowest number clones represented once

with only 29 unique clones. These results are contrasted by the results from the RFLP patterns of the background libraries from VRP9. Of the 84 total clones in library 9V and 100 total clones in library 9S, 45 and 54 clones had unique RFLP patterns, and contained no clone that was represented more than 8 times in the library. Additionally, of the 100 clones from libraries 5V and 5F, library 5V contained 43 clones, and library 5F had 54 clones with unique RFLP patterns. Thus, the 5C and 5S libraries from the petroleum impacted sediments had a higher occurrence of clones

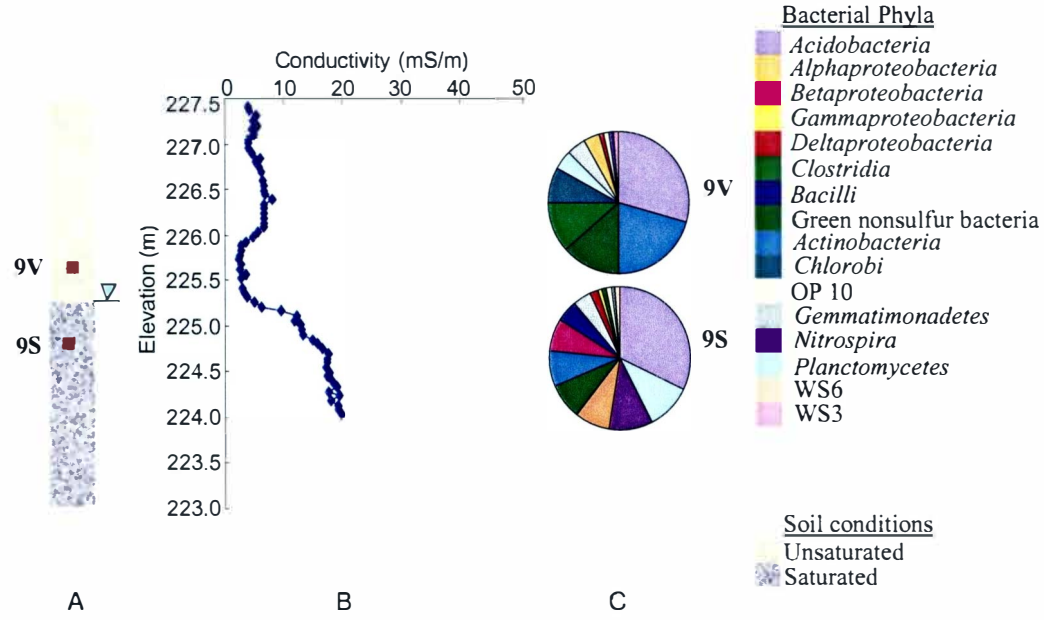

Figure 4. Soil Conditions, Conductivity Profile, and Microbial Community Composition of the Background Site (VRP9). The bar diagram (A) shows the unsaturated and water saturated sediments, and (B) the vertical sediment conductivity profile is shown. Pie charts show the microbial community composition for the sediments from the vadose zone (9V), and water saturated sediments (9S) (C). The triangle symbol denotes the level of the ground water table, and the red squares denote the sampling depths for the clone libraries.

with identical RFLP patterns whereas all other libraries had a lower occurrence of clones with identical RFLP patterns.

Shannon-Weiner diversity indices calculated from the results of the RFLP patterns revealed that the microbial communities from non-petroleum impacted zones at the contaminated location (5V, 5F) and from the background location (9V, 9S) had higher diversity ($H' > 3.92$) and evenness ($J > 0.95$) (Table 1). In contrast, microbial communities from the petroleum impacted sediments (5C, and 5S) showed lower diversity ($H' < 3.78$) and evenness ($J < 0.92$) (Table 1).

Table 1

Summary of the16S rRNA Gene Libraries from the Carson City Site

Location	Sample	Elevation (m)	Total # clones	# of clones sequenced	Shannon Weiner Index	
					H'	*J*
VRP5	5V	226.93	100	62	3.92	0.95
	5F	225.85	100	68	4.03	0.96
	5C	224.93	97	61	3.78	0.92
	5S	224.31	95	46	3.40	0.89
VRP9	9V	225.85	84	60	3.95	0.96
	9S	224.93	100	68	4.00	0.95

Phylogenetic Analysis

All unique clones determined by RFLP plus a single representative clone from each of the identical RFLP groups were used for DNA sequencing and phylogenetic analysis. Pie charts representing the microbial community composition by microbial phylum for each sample depth as determined by 16S gene sequencing are presented in Figure 3C for the contaminated site, and in Figure 4C for the uncontaminated site.

Phylogenetic analysis of partial 16S rDNA sequences revealed a diverse microbial community in each of the different sampling depths from the sediments within the contaminated and uncontaminated locations (Table 2).

In the upper vadose sediments from the VRP5 contaminated site (library 5V), the most abundant (54%) 16S rRNA gene sequences were highly similar to several groups of uncultured *Acidobacteria* (54 clones) (Fig. 5A), while 19 out of the 100 total 5V clones were over 98% identical to an uncultured *Chloroflexi* clone of the green nonsulfur bacteria (Fig. 5B), both commonly detected in forest soils (Janssen, 2006; Rappe & Giovannoni, 2003). The *α-Proteobacteria* subdivision comprised 11% of the 5V microbial community (Table 2) with a large proportion of those sharing over 98% identity to the methanotrophic *Methylocapsa acidiphila* (7 clones) (Fig. 5C). A large methanotrophic population was also found in the 5F library with sequences sharing over 98% identity to *M. acidiphila* (18 clones) and *Hyphomicrobium methylovorum* (8 clones) (Fig. 5C). However, the most abundant clones in the 5F library were over 98% identical to the aromatic hydrocarbon degrading *Brachymonas petroleovorans* (21 clones) of the *β-Proteobacteria* subdivision. Also 7 out of the 100 5F clones shared high sequence identity to the aromatic hydrocarbon degrading *Sphingomonas aromaticivorans* of the *α-Proteobacteria,* indicating that known aromatic hydrocarbon degrading populations comprised 28% of the entire 5F microbial community (Fig. 5C). Three clones in both the 5V and 5F libraries were greater than 95% identical to *Beggiatoa alba* within the *γ-Proteobacteria*, which is a known sulfide oxidizing bacterium. The remainder of sequences from libraries 5V and 5F were similar to common soil microbiota from the *δ-Proteobacteria*, *Clostridia, Bacilli*, *Planctomycetes*, *Actinobacteria*, and OP10 divisions (Table 2, Fig. 5C, D, and E).

In the contaminated zone (5C) and water saturated zone (5S), the most common 16S rRNA gene sequences detected included species within the *δ-Proteobacteria* (22%) and green nonsulfur bacteria (18%) (Table 2). Twenty-one out of the total 97 clones from library 5C as well as 31 out of the 95 total clones from library 5S were over 98% identical to the syntrophic bacterium *Syntrophus* sp. B2 of the *δ-Proteobacteria* subdivision (Fig. 5C). Members of the genus *Syntrophus* convert the organic acid intermediates of anaerobic hydrocarbon degradation such as propionate, acetate, and butyrate into CO_2, H_2, and formate, which in turn are utilized by hydrogenotrophic organisms, such as methanogens. Thus, the presence of syntrophic species such as *Syntrophus* is a common indicator of methanogenesis (Schink, 1997). Fifteen clones from 5C and a single clone from 5S were closely related (> 98%) to the uncultured clone WCHB1-05 from petroleum contaminated sediments at the former Wurtsmith Airforce Base (AFB) (Dojka *et al.*, 1998), while 15 clones from 5S were 98% identical to the uncultured clone TA17 from a terephthalate-degrading anaerobic granular sludge system (Wu *et al.*, 2001), both clustering within the green nonsulfur division (Fig. 5B). Ten out of the 97 total clones from library 5C shared over 98% identity to the Wurtsmith clone WCHB1-77, which grouped with 95% identity to the sulfate reducing bacteria *Desulfosporosinus* of the *Clostridia* division (Fig. 5D). There were also smaller *Clostridia* populations from library 5C (2 clones) and 5S (4 clones) which were 98% identical to the syntrophic *Pelotomaculum*, while three clones from the 5C library were related to *Clostridium cellobioparum*, and one 5C clone was related *Clostridium nitrophenolicum* (Fig. 5D). Three clones from the 5C library and 6 clones from the 5S library shared over 98% similarity to several genera within the *Bacteroidetes* division (Fig. 5E), while two clones from the 5C library also shared high sequence

identity (>98%) with the known hydrocarbon degrading, dissimilatory iron reducing *Rhodoferax ferrireducens* of the *β-Proteobacteria* (Fig. 5C). There were also several phyla which were detected exclusively in the 5C and 5S libraries representing the contaminated zones including the *Spirochetes*, OP5, and OP8 divisions (Table 2). In addition, unique to library 5C were also clones from the OP11 and *ε-Proteobacteria* divisions (Table 2).

To compare the microbial community from petroleum contaminated sediments with increased conductivity to the microbial community from background sediments with lower conductivity values, 16S rRNA gene libraries were also constructed from the VRP9 uncontaminated background site. The most abundant clones from the upper vadose background sediments (9V) (29%) were identical to several groups of uncultured *Acidobacteria* clones detected in the 5V libraries from the vadose sediments of the contaminated site (Fig. 5A). These were also the most abundant clones (32%) detected within the water saturated 9S sediments (Table 2). Twenty-three percent of the 9V sequences shared high identity with groups of *Actinobacteria* clones commonly detected in natural sediments (Table 2, Fig. 5E). Ten out of the 84 total 9V clones clustered within the *Clostridia* division, with 7 clones related to *Anaerovibrio glycerini* and three related to *Desulfosporosinus* as found in the 5C library (Fig. 5D). Additionally 11% of the 9V sequences were affiliated with several *Chloroflexi* clones from within the green nonsulfur division; however, these were of a

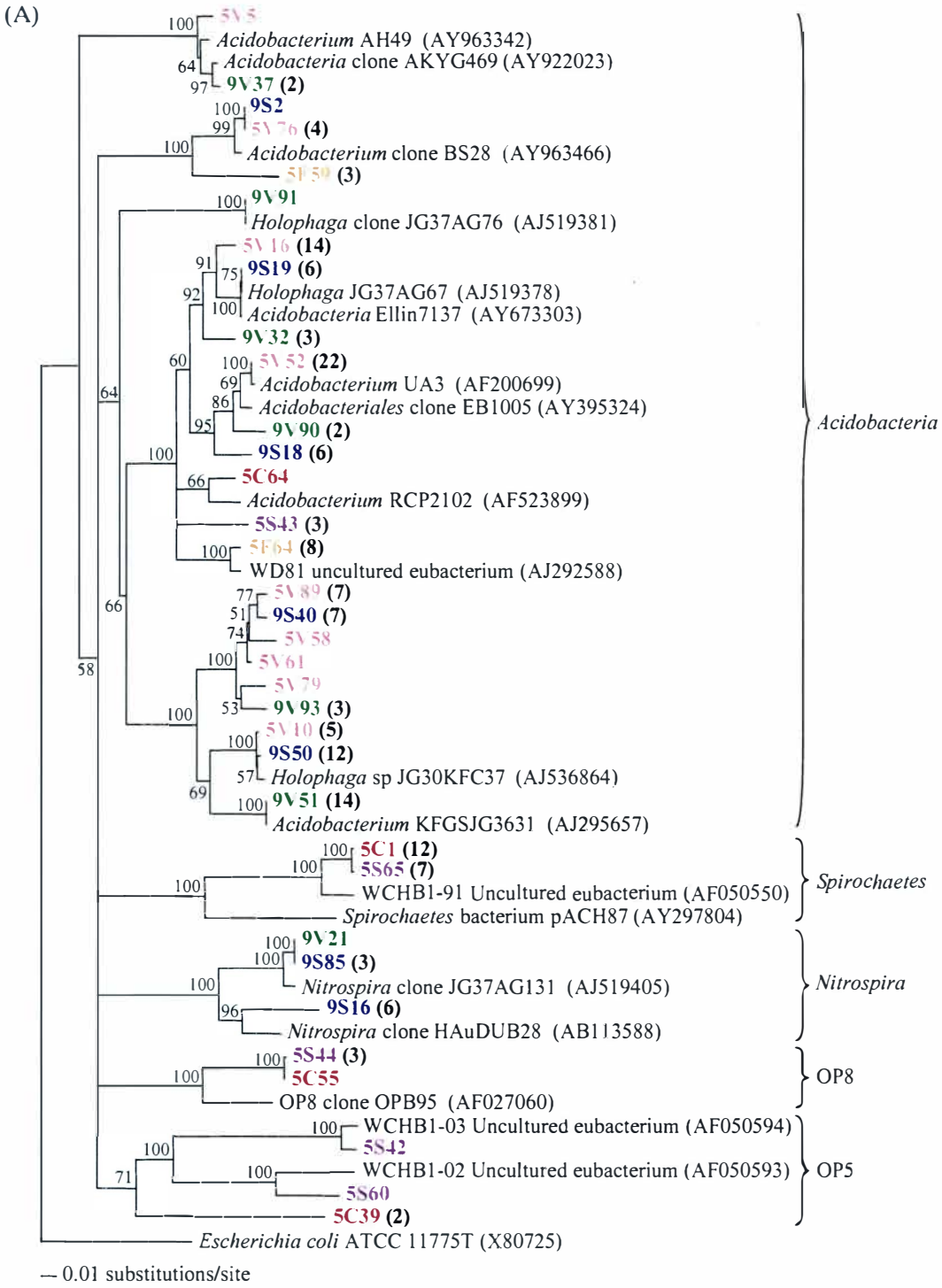
(A)
Acidobacterium AH49 (AY963342)
Acidobacteria clone AKYG469 (AY922023)
9V37 (2)
9S2
Acidobacterium clone BS28 (AY963466)
(3)
9V91
Holophaga clone JG37AG76 (AJ519381)
(14)
9S19 (6)
Holophaga JG37AG67 (AJ519378)
Acidobacteria Ellin7137 (AY673303)
9V32 (3)
(22)
Acidobacterium UA3 (AF200699)
Acidobacteriales clone EB1005 (AY395324)
9V90 (2)
9S18 (6)
5C64
Acidobacterium RCP2102 (AF523899)
5S43 (3)
(8)
WD81 uncultured eubacterium (AJ292588)
(7)
9S40 (7)
9V93 (3)
(5)
9S50 (12)
Holophaga sp JG30KFC37 (AJ536864)
9V51 (14)
Acidobacterium KFGSJG3631 (AJ295657)
5C1 (12)
5S65 (7)
WCHB1-91 Uncultured eubacterium (AF050550)
Spirochaetes bacterium pACH87 (AY297804)
9V21
9S85 (3)
Nitrospira clone JG37AG131 (AJ519405)
9S16 (6)
Nitrospira clone HAuDUB28 (AB113588)
5S44 (3)
5C55
OP8 clone OPB95 (AF027060)
WCHB1-03 Uncultured eubacterium (AF050594)
5S42
WCHB1-02 Uncultured eubacterium (AF050593)
5S60
5C39 (2)
Escherichia coli ATCC 11775T (X80725)
0.01 substitutions/site
Acidobacteria
Spirochaetes
Nitrospira
OP8
OP5

Figure 5A

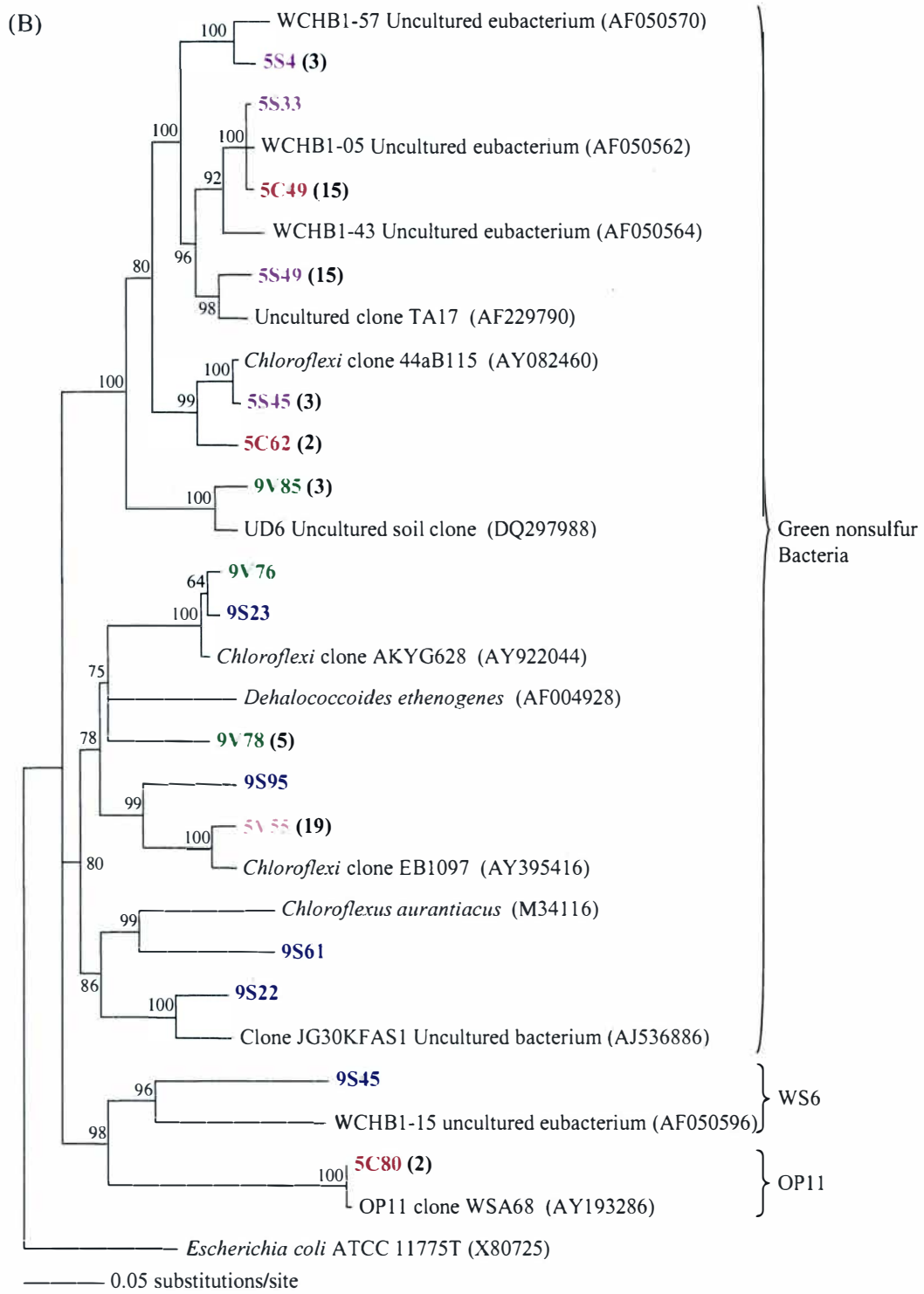
(B)
WCHB1-57 Uncultured eubacterium (AF050570)
5S4 (3)
5S33
WCHB1-05 Uncultured eubacterium (AF050562)
5C49 (15)
WCHB1-43 Uncultured eubacterium (AF050564)
5S49 (15)
Uncultured clone TA17 (AF229790)
Chloroflexi clone 44aB115 (AY082460)
5S45 (3)
5C62 (2)
9V85 (3)
UD6 Uncultured soil clone (DQ297988)
9V76
9S23
Chloroflexi clone AKYG628 (AY922044)
Dehalococcoides ethenogenes (AF004928)
9V78 (5)
9S95
5V55 (19)
Chloroflexi clone EB1097 (AY395416)
Chloroflexus aurantiacus (M34116)
9S61
9S22
Clone JG30KFAS1 Uncultured bacterium (AJ536886)
9S45
WCHB1-15 uncultured eubacterium (AF050596)
5C80 (2)
OP11 clone WSA68 (AY193286)
Escherichia coli ATCC 11775T (X80725)
0.05 substitutions/site
Green nonsulfur Bacteria
WS6
OP11

Figure 5B

(C)

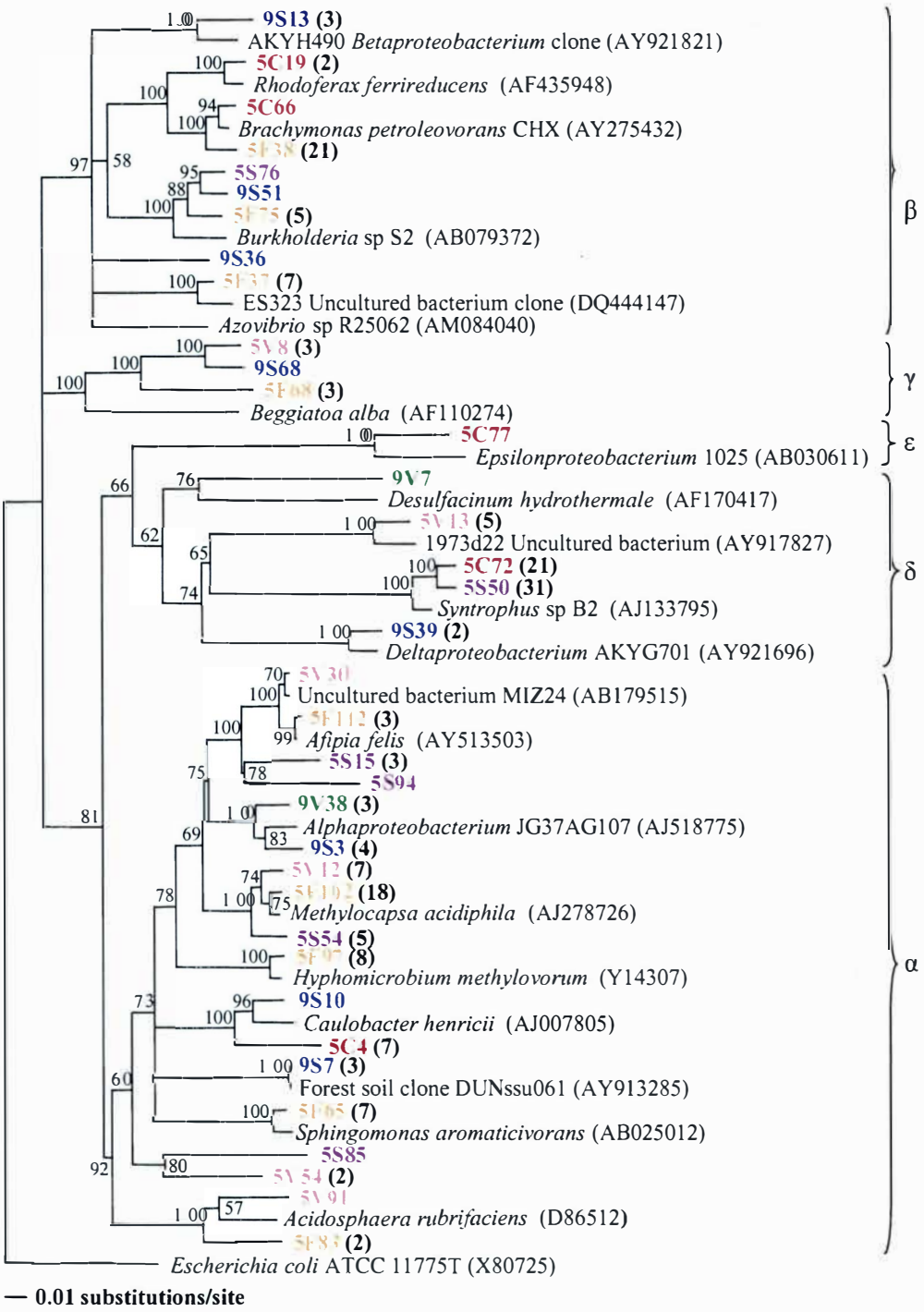
9S13 (3)
AKYH490 Betaproteobacterium clone (AY921821)
5C19 (2)
Rhodoferax ferrireducens (AF435948)
5C66
Brachymonas petroleovorans CHX (AY275432)
5E38 (21)
5S76
9S51
5E75 (5)
Burkholderia sp S2 (AB079372)
9S36
5E37 (7)
ES323 Uncultured bacterium clone (DQ444147)
Azovibrio sp R25062 (AM084040)
5V8 (3)
9S68
5E68 (3)
Beggiatoa alba (AF110274)
5C77
Epsilonproteobacterium 1025 (AB030611)
9V7
Desulfacinum hydrothermale (AF170417)
5V13 (5)
1973d22 Uncultured bacterium (AY917827)
5C72 (21)
5S50 (31)
Syntrophus sp B2 (AJ133795)
9S39 (2)
Deltaproteobacterium AKYG701 (AY921696)
5V30
Uncultured bacterium MIZ24 (AB179515)
5E112 (3)
Afipia felis (AY513503)
5S15 (3)
5S94
9V38 (3)
Alphaproteobacterium JG37AG107 (AJ518775)
9S3 (4)
5V12 (7)
5E102 (18)
Methylocapsa acidiphila (AJ278726)
5S54 (5)
5E97 (8)
Hyphomicrobium methylovorum (Y14307)
9S10
Caulobacter henricii (AJ007805)
5C4 (7)
9S7 (3)
Forest soil clone DUNssu061 (AY913285)
5E65 (7)
Sphingomonas aromaticivorans (AB025012)
5S85
5V54 (2)
5V91
Acidosphaera rubrifaciens (D86512)
5E83 (2)
Escherichia coli ATCC 11775T (X80725)
β
γ
ε
δ
α
— 0.01 substitutions/site

Figure 5C

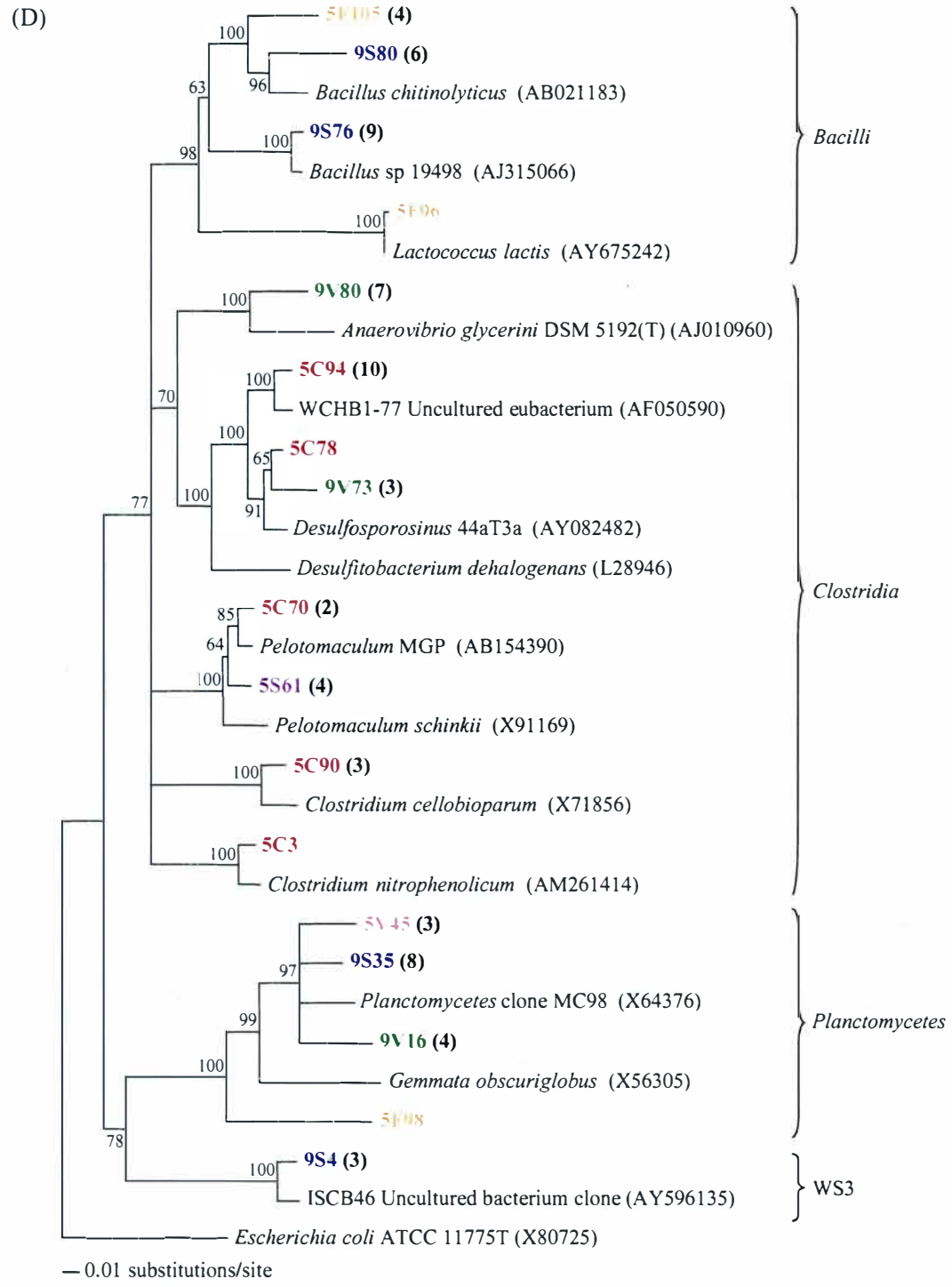
(D)
5V105 (4)
9S80 (6)
Bacillus chitinolyticus (AB021183)
9S76 (9)
Bacillus sp 19498 (AJ315066)
5F06
Lactococcus lactis (AY675242)
Bacilli
9V80 (7)
Anaerovibrio glycerini DSM 5192(T) (AJ010960)
5C94 (10)
WCHB1-77 Uncultured eubacterium (AF050590)
5C78
9V73 (3)
Desulfosporosinus 44aT3a (AY082482)
Desulfitobacterium dehalogenans (L28946)
5C70 (2)
Pelotomaculum MGP (AB154390)
5S61 (4)
Pelotomaculum schinkii (X91169)
5C90 (3)
Clostridium cellobioparum (X71856)
5C3
Clostridium nitrophenolicum (AM261414)
Clostridia
5V45 (3)
9S35 (8)
Planctomycetes clone MC98 (X64376)
9V16 (4)
Gemmata obscuriglobus (X56305)
5F08
Planctomycetes
9S4 (3)
ISCB46 Uncultured bacterium clone (AY596135)
WS3
Escherichia coli ATCC 11775T (X80725)
0.01 substitutions/site

Figure 5D

(E)

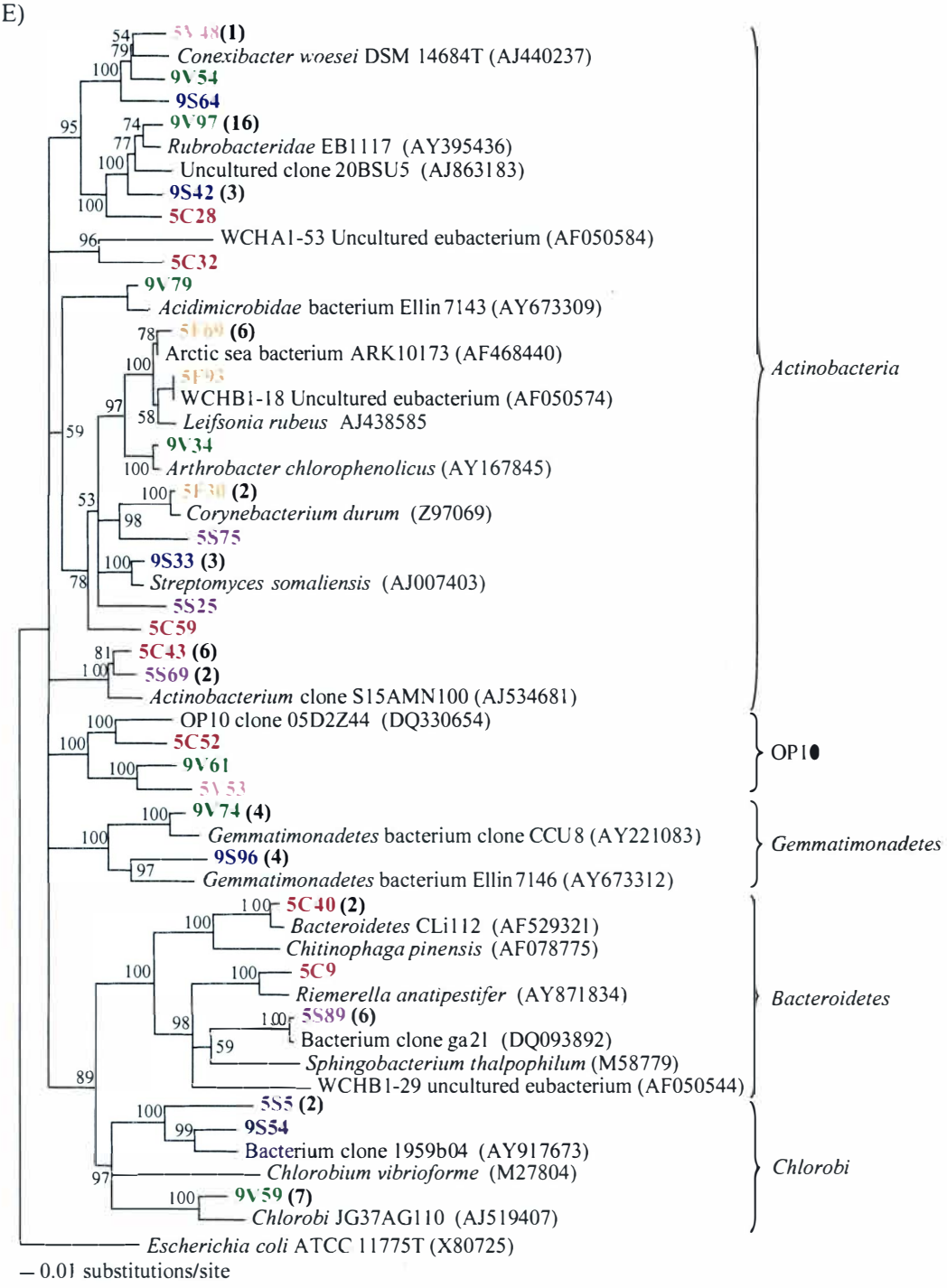
5V48(1)
Conexibacter woesei DSM 14684T (AJ440237)
9V54
9S64
9V97 (16)
Rubrobacteridae EB1117 (AY395436)
Uncultured clone 20BSU5 (AJ863183)
9S42 (3)
5C28
WCHA1-53 Uncultured eubacterium (AF050584)
5C32
9V79
Acidimicrobidae bacterium Ellin7143 (AY673309)
5V69 (6)
Arctic sea bacterium ARK10173 (AF468440)
5F93
WCHB1-18 Uncultured eubacterium (AF050574)
Leifsonia rubeus AJ438585
9V34
Arthrobacter chlorophenolicus (AY167845)
5F30 (2)
Corynebacterium durum (Z97069)
5S75
9S33 (3)
Streptomyces somaliensis (AJ007403)
5S25
5C59
5C43 (6)
5S69 (2)
Actinobacterium clone S15AMN100 (AJ534681)
OP10 clone 05D2Z44 (DQ330654)
5C52
9V61
5V53
9V74 (4)
Gemmatimonadetes bacterium clone CCU8 (AY221083)
9S96 (4)
Gemmatimonadetes bacterium Ellin7146 (AY673312)
5C40 (2)
Bacteroidetes CLi112 (AF529321)
Chitinophaga pinensis (AF078775)
5C9
Riemerella anatipestifer (AY871834)
5S89 (6)
Bacterium clone ga21 (DQ093892)
Sphingobacterium thalpophilum (M58779)
WCHB1-29 uncultured eubacterium (AF050544)
5S5 (2)
9S54
Bacterium clone 1959b04 (AY917673)
Chlorobium vibrioforme (M27804)
9V59 (7)
Chlorobi JG37AG110 (AJ519407)
Escherichia coli ATCC 11775T (X80725)
0.01 substitutions/site
Actinobacteria
OP10
Gemmatimonadetes
Bacteroidetes
Chlorobi

Figure 5E

Figure 5. Evolutionary Distance Dendrograms of Bacterial 16S rRNA Gene Sequence Types Obtained from the Carson City Sediments. Phylogenetic divisions are listed outside the brackets: (A) *Acidobacteria, Spirochaetes, Nitrospira,* OP8, and OP5 (B) Green nonsulfur bacteria, WS6, and OP11 (C) *α-, β-, γ-, δ-,* and *ε-Proteobacteria*; (D) *Bacilli, Clostridia, Planctomycetes*, and WS3; (E) *Actinobacteria*, OP10, *Gemmatimonadetes, Bacteroidetes,* and *Chlorobi. E. coli* (X80725) was used as an out-group for all trees. Reference sequences were chosen from the Ribosomal Database Project and NCBI database. Clones from the separate libraries are color coded as 5V (pink), 5F (orange), 5C (red), 5S (purple), 9V (green), and 9S (blue). The total number of clones for each sequence type is shown in parenthesis except for those sequence types with only one representative. Branch points supported by neighbor-joining distance analysis (bootstrap values, >50%) are shown.

completely different group than the green nonsulfur clones detected within the 5C and 5S libraries from the contaminated sediment (Fig. 5B). Additionally, both the 9V and 9S 16S rRNA gene libraries showed high diversity containing common soil microbes from within the *α-*, *β-*, *γ-*, and *δ-Proteobacteria* subdivisions, as well as the *Planctomycetes* and *Chlorobi* phyla (Table 2). Furthermore, there were several populations detected only in the VRP9 background sediments with high sequence identity to uncultured forest soil clones from within the *Gemmatimonadetes*, *Nitrospira* (Fig. 5E, A). Exclusively found only in library 9S were clones from the *WS3* and *WS6* phyla (Table 2). In general, over 61% of the clones from the 16S rRNA gene libraries were related at the species level to published sequences (> 97% sequence identity), 19% were related at the level of the genus similarity (> 95% identity), 19% shared family similarity (> 90% identity), and less than 1% were only identical at the level of phyla (> 80% identity). Thus, no new phylogenetic divisions were detected at the Carson City site.

Table 2

Microbial Composition of the 16S rRNA Gene Libraries from the Carson City Site

Phylogenetic class	Percent composition					
	5V	5F	5C	5S	9V	9S
Acidobacteria	54	12	2	6	29	32
Green nonsulfur	19	-	18	23	11	4
Alphaproteobacteria	11	39	7	10	4	9
Deltaproteobacteria	5	-	22	33	1	2
Clostridia	3	-	17	4	12	1
Gammaproteobacteria	3	3	-	-	-	1
Planctomycetes	3	1	-	-	5	9
Actinobacteria	1	9	7	4	23	9
OP10	1	-	1	-	1	-
Betaproteobacteria	-	34	3	1	-	5
Bacilli	-	2	-	-	-	8
Gemmatimonadetes	-	-	-	-	5	4
Nitrospira	-	-	-	-	1	11
WS3	-	-	-	-	-	3
WS6	-	-	-	-	-	1
Chlorobi	-	-	-	2	8	1
Bacteroidetes	-	-	4	6	-	-
Spirochetes	-	-	11	8	-	-
OP5	-	-	2	2	-	-
OP8	-	-	3	1	-	-
OP11	-	-	2	-	-	-
Epsilonproteobacteria	-	-	1	-	-	-

In order to determine if the microbial community composition for each of the sample locations was significantly different, the Libshuff program was used (Singleton *et al.*, 2001). Libshuff calculated *p*-values of less than 0.05 are considered to be an indication of significant difference. For the six libraries from the contaminated and uncontaminated locations, Libshuff pairwise comparisons revealed significant differences among all libraries with calculated *p*-values < 0.001 for most comparison, but with $p=0.007$ for the comparison 5S vs. 5C, $p=0.002$ for 9S vs. 5V,

and p=0.003 for 9S vs. 9V (Table 3).

Table 3

Libshuff Calculated p-values from Carson City 16S rRNA Gene Library Comparisons

Homologous (X)	Heterologous (Y)					
	5V	5F	5C	5S	9V	9S
5V	1	0.001	0.001	0.001	0.001	0.001
5F	0.001	1	0.001	0.001	0.001	0.001
5C	0.001	0.001	1	0.001	0.001	0.001
5S	0.001	0.001	0.007	1	0.001	0.001
9V	0.001	0.001	0.001	0.001	1	0.001
9S	0.002	0.001	0.001	0.001	0.003	1

Libshuff coverage plots of the two most extreme 16S rRNA gene library comparisons are shown in Figure 6. The large gap in homologous vs. heterologous coverage values as seen in comparisons between libraries 5C versus 9V (Fig. 6A) represents significant differences in the microbial community between the two sample sites. Similar coverage curves were observed for comparisons between the 5C and 5S libraries versus all other 16S rRNA gene libraries from VRP5 and VRP9 (data not shown). In contrast, the coverage curve for comparison of libraries 5S versus 5C revealed a greater similarity between these two libraries than with any other comparison, suggesting that the two libraries, although significantly different, do contain some similar deep taxa (Fig. 6B). These results demonstrate that the microbial communities from each of the different sampling elevations representing the different geoelectrical zones are significantly different, and suggest that the observed geophysical differences may be due to the microbial activity of distinct populations within these zones.

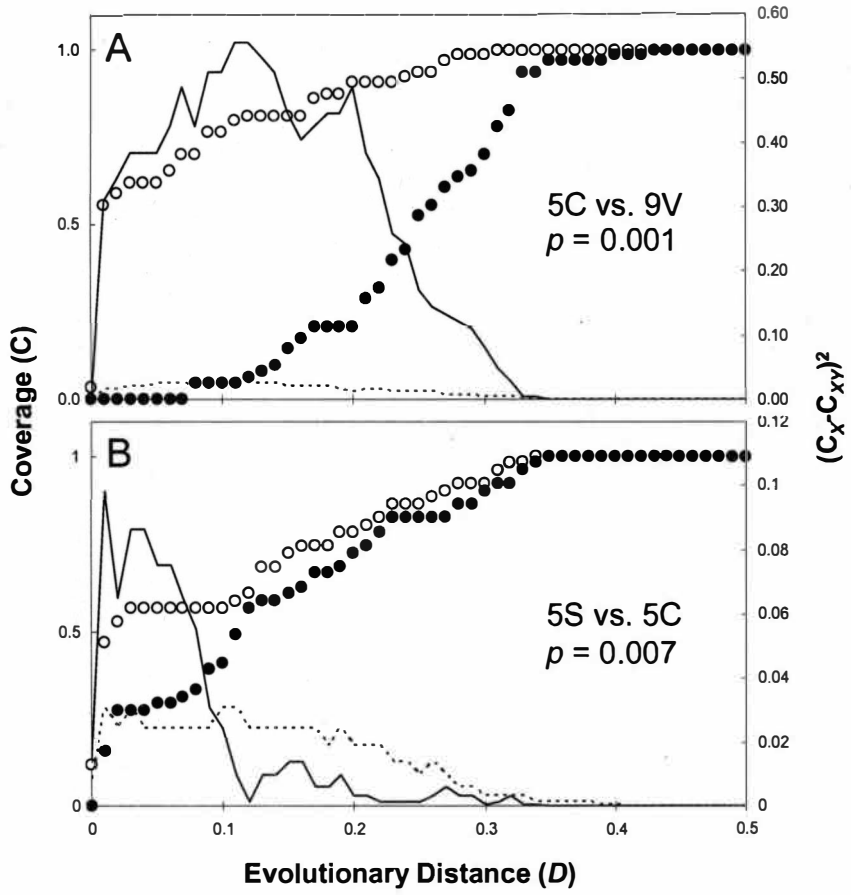

Figure 6. Libshuff 16S rRNA Gene Library Analysis. Comparison of the 16S rRNA gene sequence libraries 5C vs. 9V (A), and 5C vs. 5S (B) representing the two most extreme library comparisons. Homologous (C_x, open circles) and heterologous (C_{xy}, closed circles) coverage curves are given for each comparison. Solid lines indicate the square of the difference between the homologous and heterologous libraries $(C_x–C_{xy})^2$ for the samples at each evolutionary distance (D) value. Dashed lines indicate the same $(C_x–C_{xy})^2$ values for p = 0.05 (level at which libraries X and Y are considered significantly different).

Discussion

Few studies have investigated the biological impact on subsurface geophysical properties (Atekwana *et al.*, 2004b; Atekwana *et al.*, 2005; Atekwana, 2003; Duris, 2002), and none to date has completed an in-depth characterization of the microbial

community structure in petroleum contaminated sediments associated with anomalously high conductivity readings. Previous work at the Carson City site revealed an increase in the proportion of culturable hydrocarbon degrading microbes in the free phase LNAPL zone, where the highest conductivity values were recorded (Duris, 2002). Additionally, culture-independent RISA profiles demonstrated changes in the overall microbial community structure, which paralleled changes in LNAPL contamination and bulk electrical conductivity (Duris, 2002). These methods were quite useful for investigating overall structural changes in the microbial community; however, they were unable to characterize the specific microbial populations from within the contaminated and background sites. A detailed understanding of the complex biogeophysical relationships existing in the contaminated subsurface requires knowledge into the specific makeup of the biological community so that the interactions at the biophysicochemical level, and the ways in which organisms modify and respond to changes in their environments can be determined (Newman & Banfield, 2002). Therefore, we conducted an in-depth characterization of the microbial community structure using 16S rRNA gene cloning and sequencing from samples collected within zones of higher and lower conductivity in petroleum contaminated and background sites. In addition, we measured the subsurface conductivity in both the contaminated and background sites in order to evaluate the microbiological impact on subsurface geophysical properties in petroleum contaminated sediments.

Analysis of the microbial community structure from the Carson City site revealed that the subsurface geophysical signatures observed in the contaminated and background sites paralleled changes in both petroleum contamination and microbial composition. In sediments of low electrical conductivity, as in the VRP9 background

sediments and vadose sediments from the VRP5 contaminated site (Fig. 3B, 4B), the microbial communities were dominated by members of the *Acidobacteria* phylum (Barns *et al.*, 1999), as well as by other commonly associated subsurface microbiota including the *Planctomycetes*, *Gemmatimonadetes*, and *Nitrospira* phyla (Janssen, 2006). In the capillary fringe sediment represented by library 5F, where there was a slight increase in the electrical conductivity, the microbial community was dominated by aerobic, aromatic hydrocarbon degrading populations. This would be expected in an aged petroleum contaminated site as the lighter, volatile fractions of hydrocarbons would rise. The finding of a large methanotrophic population in library 5F supports previous geochemical findings which had suggested that methanogenesis is occurring within the VRP5 contaminated zone (Atekwana *et al.*, 2005). Moreover, in the petroleum impacted sediments, where the highest conductivity values were recorded, the finding of a large *Syntrophus* population in libraries 5C and 5S corroborated this as well. Additionally, the presence of green nonsulfur bacteria, *Clostridia*, *Bacteroidetes*, as well as sulfate and iron reducing populations within the electrically conductive free phase contaminant zone, support geochemical findings that described anaerobic conditions within the contaminated zone (Atekwana *et al.*, 2005). Anaerobic conditions are common in aged LNAPL contaminated sediments, and are necessary for methanogenesis to occur (Banning *et al.*, 2005; Dojka *et al.*, 1998; Feris *et al.*, 2004). Thus, results of the 16S rRNA gene cloning and sequencing of different libraries demonstrate significant differences in microbial community composition spatially over a vertical subsurface gradient concomitant with changes in LNAPL contamination and electrical properties of the contaminated sediments.

Intriguingly, many of the 16S rRNA gene clones detected in the electrically conductive free phase zone (library 5C) were of high sequence similarity to clones

from a similar petroleum contaminated site at the former Wurtsmith Airforce base in Oscoda, MI (Dojka *et al.*, 1998). An in-depth characterization into the microbial community composition from that site revealed a diverse population within the contaminated sediments, which shared many similarities to the Carson City contaminated site. These included large populations of both *Syntrophus* of the *δ-Proteobacteria*, and uncultured clones of the Green nonsulfur bacteria. There were also several significant populations of fermentative microorganisms such as *Clostridia*, plus several acetogenic (acetate generating) populations of *Spirochetes*, and *Bacteroidetes*. Additionally, there were smaller populations of dissimilatory iron reducing and sulfate reducing bacteria, as well as several populations from the OP5, OP8, and OP11 divisions. The importance of the Wurtsmith site comes from a separate geophysical study performed, which first reported anomalous electrical conductivity measurements in the aged petroleum contaminated sediments (Bermejo *et al.*, 1997). Comparison of these two separate studies with our work allows for speculation that these are the microbial populations that may have the largest impact on subsurface geophysical properties in aged petroleum contaminated sediments.

Geophysical (specifically electrical conductivity) properties of the subsurface are influenced by three main components: 1, the petrophysical characteristics (i.e. sediment type, size, and interfacial or grain surface properties); 2, the amount of fluid saturation of the pore space; and 3, the fluid electrolytic (ionic strength) properties (Archie, 1942). At the former Crystal Refinery at Carson City, no changes in fluid saturation or sediment lithology (grain size/type) were found to be coincidental with changes in the bulk conductivity observed within the petroleum contaminated sediments (Atekwana *et al.*, 2000). Therefore, the geoelectrical properties of the LNAPL impacted sediments must be influenced by either changes in the electrolytic

properties of the pore fluids, the alteration of the interfacial properties of the grain surface (surface conductance), or the combined effects of both .

Microbial activity has been shown to alter the subsurface fluid electrolytic properties in LNAPL contaminated sediments (Atekwana *et al.*, 2005). Fluid conductivity of groundwater is directly controlled by the amount of total dissolved solids (TDS) (number of ions present in the solution). Organic acids produced as metabolic byproducts of hydrocarbon degradation have been shown to cause mineral dissolution resulting in the release of ions into the pore space increasing the ionic strength and thus conductivity of the pore fluid (Cozzarelli *et al.*, 1990; McMahon *et al.*, 1995; Sauck, 2000). Duris (2002) presented SEM images of highly etched sediment grains from the VRP5 contaminated zone, not observed in the background sediments, indicative of extensive mineral weathering. Etching patterns on sediment grains have been observed within multiple petroleum contaminated sites (Bennett *et al.*, 1996; Bennett *et al.*, 2001) and occur from the dissolution of the mineral surface due to a rapid exchange of charge-balancing cations (K^+, Na^+, or Ca^+) for protons at the mineral surface, releasing these cations into the surrounding pore fluid (Bennett *et al.*, 2001). Geochemical data of the petroleum contaminated VRP5 pore fluid revealed an increase in the amount of total dissolved solids (TDS) in the sediment pore water, suggesting that microbial enhanced mineral dissolution has occurred (Atekwana *et al.*, 2005). Moreover, the presence of fermentative *Clostridia* species, as well as the large *Syntrophus* population detected in this study from within the free phase contaminant zone, demonstrate the presence of microbial populations which produce organic acids such as acetate, butyrate, propionate, and fumarate further corroborating these results (Fig. 5) (Boone & Bryant, 1980; Jackson *et al.*, 1999; Soucaille & Goma, 1986). Furthermore, in a parallel study, increases in microbially

produced biosurfactants (e.g. rhamnolipids) were also detected at VRP5 in the Carson City site (Cassidy *et al.*, 2002). Biosurfactants reduce the surface tension of residual hydrocarbons on the grain surface allowing for microbial attachment, resulting in direct microbe-mineral interactions and possible further dissolution of the mineral grain (Cassidy *et al.*, 2001; Cassidy *et al.*, 2002).

The above geophysical, geochemical, and microbial data suggest that changes in fluid electrolytic properties due to microbial enhanced mineral dissolution may play an important role in altering the subsurface electrical conductance. However, Atekwana *et al.* (2005) report that the ionic strength (TDS levels) of the pore fluid could not completely explain the anomalously high conductivity readings in the free phase zone (Atekwana *et al.*, 2005). Furthermore, Abdel Aal *et al.* (2004), using geophysical methods of induced polarization to investigate the complex conductivity at the Carson City site, report that changes in the interfacial properties on the grain surface resulting in surface conductance play an important role in altering subsurface electrical conductivity. Alterations of the interfacial properties of the sediment grains can result from microbial colonization, exopolysaccharide production, microbial biofilm formation, and mineral precipitation of metal sulfides by microbial activity (Abdel Aal *et al.*, 2004). Williams et al. (2005) demonstrated that precipitation of iron sulfides onto the surface of sediment grains effectively altered their interfacial properties. Precipitation occurs from the abiotic reaction of microbially generated Fe(II) and H_2S to produce insoluble FeS, and has been shown to occur even at low sulfide concentrations (Williams *et al.*, 2005). The presence of dissimilatory iron reducing bacteria, such as *Rhodoferax ferrireducens*, and sulfate reducing bacteria, such as *Desulfosporosinus,* in the contaminant zone would suggest that iron and sulfate reduction is occurring in the anaerobic contaminated sediments (Finneran *et*

al., 2003; Robertson *et al.*, 2001). Furthermore, the presence of the sulfide oxidizing *Beggiatoa* in the upper sediments suggests that H_2S is escaping from the lower sediments and is utilized by the *Beggiatoa* (Fig. 5)(Schmidt *et al.*, 1987).

In conclusion, we have demonstrated that significant changes occur in the microbial community structure vertically within the sediment layers which parallel changes in the zones of petroleum contamination and in the geoelectrical properties of those sediment zones. The low conductivity readings of the background sediments were concomitant with diverse populations of common soil microbes. Conversely, the composition of the microbial community found in the electrically conductive petroleum contaminated sediments was consistent with microbial community compositions of perturbed sites found in other petroleum contaminated locations including the presence of significant populations of fermentors, DIRB, SRB, and syntrophic bacteria (Dojka *et al.*, 1998). We speculate that the anomalous increase in electrical conductivity detected in the free phase petroleum zone was attributable to the activity of these microbial populations altering both the electrolytic properties of the pore fluid and interfacial properties of the sediment grains under the anaerobic, carbon- and electron donor-rich environmental conditions.

CHAPTER IV

LABORATORY COLUMN STUDY

Results

Geoelectrical Measurements

To investigate the spatial and temporal biogeophysical relationships in petroleum-contaminated sediments, laboratory scale mesocolumns were constructed to replicate the following field conditions: 1, a contaminated field site with an underground petroleum plume floating on top of the groundwater table (Fig. 7A); and 2, a background site without diesel contamination (Fig. 8A) (see Materials and Methods for column construction).

The bulk electrical conductivity of the column sediments was monitored over an 18 month period for both the contaminated (Fig. 7) and control (Fig. 8) columns. For both the contaminated and uncontaminated columns, large decreases in the conductivity above the water table (45 cm depth) occurred over the first three months. The lowest conductivity values recorded in the contaminated column occurred at the three month sampling point, and thus fold change in conductivity was calculated for both the contaminated and control columns as compared to the three month sampling point. Both the contaminated (Fig. 7B) and the control (Fig. 8B) columns showed an overall decrease in conductivity over the first three months in the unsaturated sediments, with the largest 3.5 fold decrease occurring at around 30 cm depth.

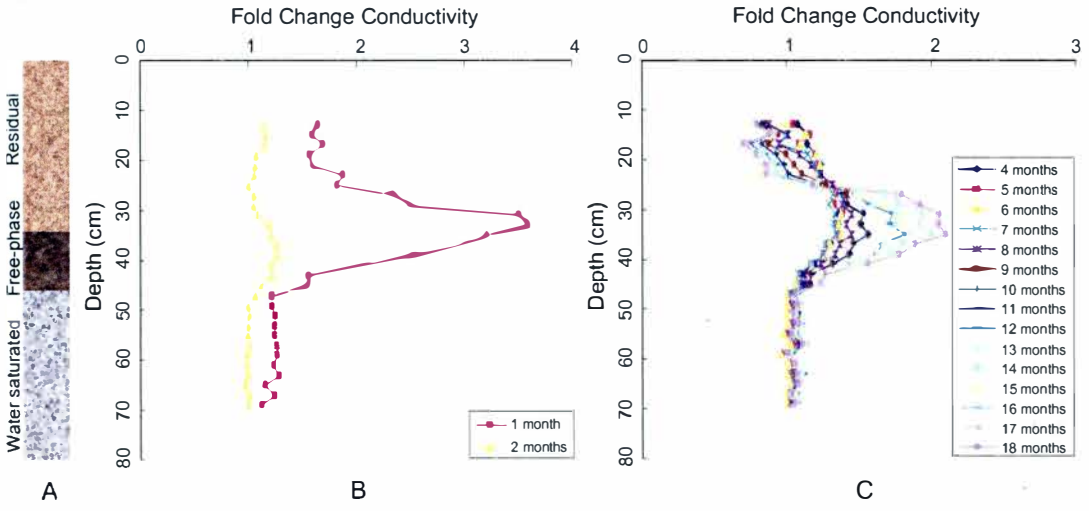

Figure 7. Soil Conditions and Conductivity Profile for the Contaminated Column. The level of LNAPL saturation is shown (A) for the residual, free, and dissolved LNAPL phases. The fold change in conductivity as compared to the conductivity values of the 3rd month is shown for the first 2 months (B), and subsequent months 4 through 18 (C).

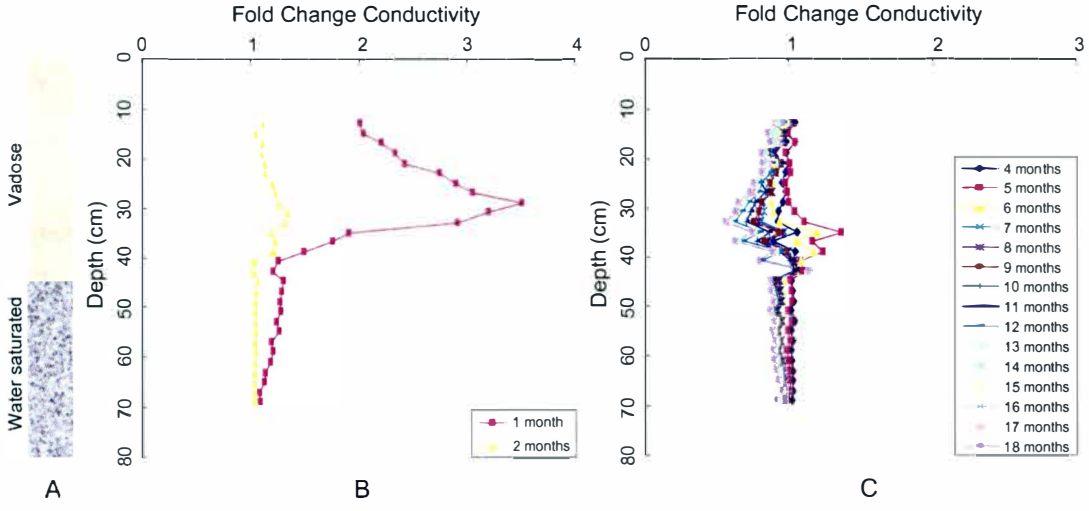

Figure 8. Soil Conditions and Conductivity Profile for the Uncontaminated Column. The level of water saturation is shown (A) for the unsaturated, and water saturated sediments. The fold change in conductivity as compared to the conductivity values of the 3rd month is shown for the first 2 months (B), and subsequent months 4 through 18 (C).

This reflects an equilibration period within the artificial environment of the columns in which the unsaturated sediments experienced drying after the initial inoculation. For both the contaminated and uncontaminated columns there was little change in the conductivity of the saturated sediments (below 45 cm) during this same time period (Fig. 7B, 8B). In the subsequent months, the conductivity of the contaminated column revealed dramatic increases within the petroleum impacted zones (Fig. 7C), with the largest change occurring within the 25 cm to 45 cm depths (> 2 fold increase). In contrast, the conductivity of the control column continued to decrease over time, most notably in the unsaturated sediments above the water table (Fig. 8C).

Most Probable Number Analysis

The number of hydrocarbon degrading microorganisms was determined for both columns along a vertical gradient using a Most Probable Number (MPN) approach. Figure 9 shows the MPN of hydrocarbon degrading microbes per gram soil in the contaminated column over the 20 month sampling period. One month after construction of the columns, the number of hydrocarbon degrading organisms was highest within the dissolved hydrocarbon zone at the 50 cm depth, reaching 460,500 MPN/g soil. During the second month the number of hydrocarbon degrading microbes increased to an overall peak value of 800,000 MPN/g soil within the same zone. Subsequent sampling dates revealed high enrichments of hydrocarbon degrading microbes in the upper sediments. At the 12 month sampling date the number of hydrocarbon degrading microbes reached approximately 956,500 MPN/g soil at the 15 cm depth, and 941,000 MPN/g soil at the 35 cm depth by the 20^{th} month. This could represent degradation of both residual hydrocarbons as well as the

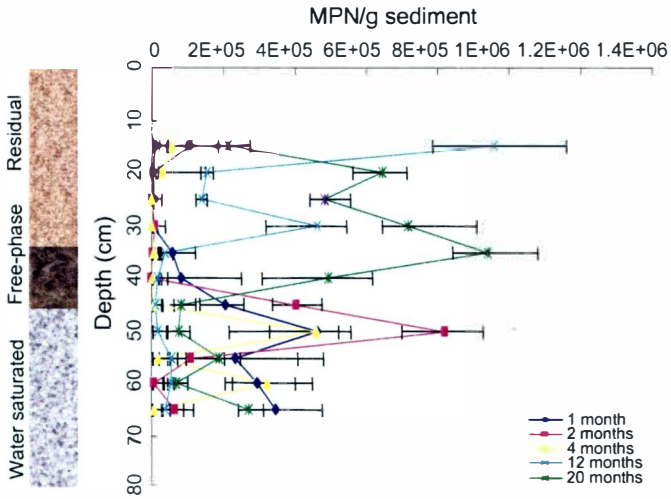

Figure 9. The Hydrocarbon Degrading Population within the Contaminated Column. The number of hydrocarbon degrading bacteria (MPN/g soil) throughout the entire column is shown for 5 sampling dates over a 20 month sampling period. Error Bars represent 95% confidence levels. The results are shown in relation to the level of LNAPL contamination in the column.

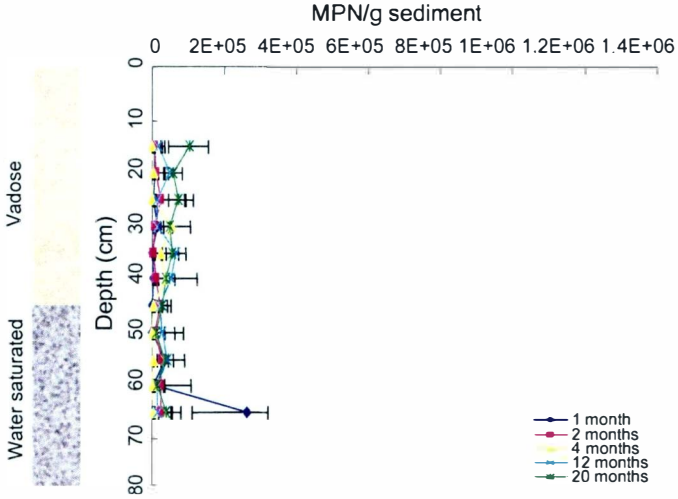

Figure 10. The Hydrocarbon Degrading Population within the Control Column. The number of hydrocarbon degrading bacteria (MPN/g soil) throughout the entire column is shown for 5 sampling dates over a 20 month sampling period. Error Bars represent 95% confidence levels. The results are shown in relation to the background conditions in the control column.

volatile fractions.

In contrast, in the control column the highest number of hydrocarbon degrading bacteria was measured during the first month sampling date reaching approximately 260,000 MPN/g soil at the 65 cm depth (Fig. 10). At all other sample dates, the number of hydrocarbon degrading microbes remained below 200,000 MPN/g soil.

Ribosomal Intergenic Spacer Analysis

Because only a small percentage of microorganisms can be cultured in the laboratory, culture-independent methods provide an opportunity to study the microbial community structure in more detail. In order to determine spatial and temporal changes in the overall microbial community structure, ribosomal intergenic spacer analysis (RISA) was performed using DNA purified from sediment samples collected over a vertical gradient within both columns at multiple time points. RISA utilizes the polymerase chain reaction (PCR) to amplify the intergenic region of the bacterial chromosome between the highly conserved 16S and 23S rRNA genes. This region tends to be highly variable in size because of different tRNA genes inserted into the region by different microbial species (Ranjard et al., 2000). Because of the variability in the intergenic region, changes in the microbial community structure can be easily resolved by analysis of changing banding patterns. The results of the RISA are shown in Figure 11 for the contaminated (Fig. 11A) and control (Fig. 11B) columns.

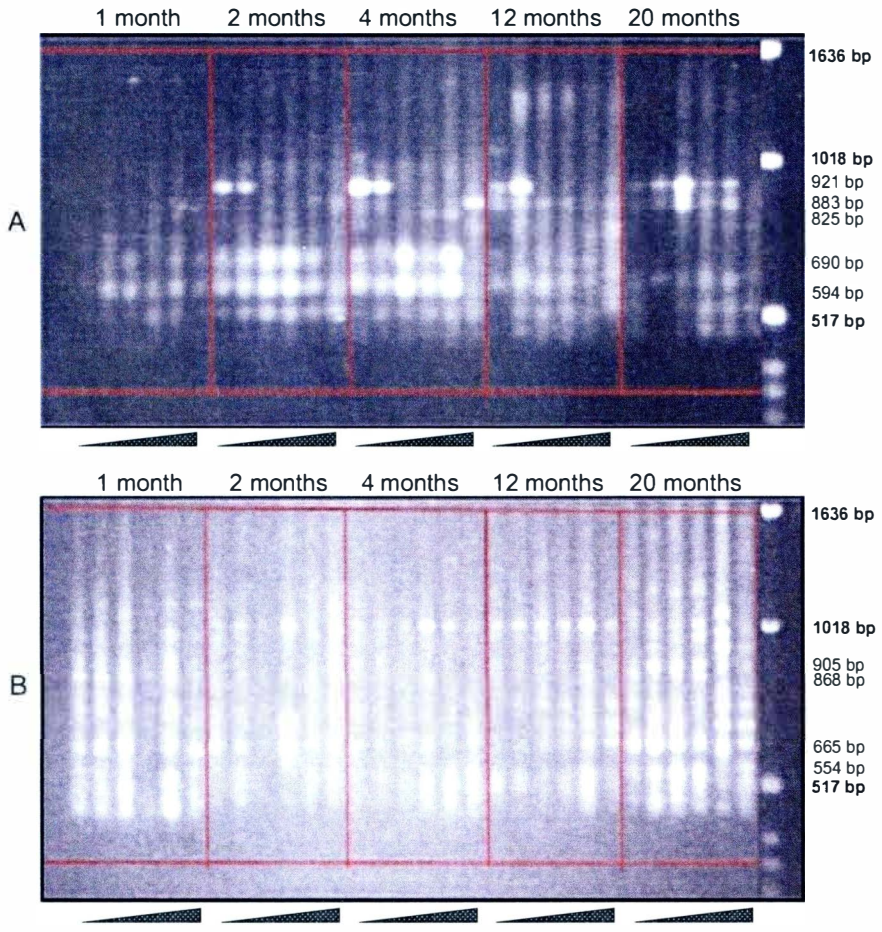

Figure 11. RISA Profiles of Laboratory Columns. Results of the RISA analysis for the contaminated (A) and control (B) columns are given for the 5 sampling dates over a 20 month period. Within each main sampling date (1, 2, 4, 12, and 20 months) the six lanes represent increasing sampling depths within the column: 15 cm, 25 cm, 35 cm, 45 cm, 55 cm, and 65 cm. A 1kb DNA ladder was used with the marker sizes of 1636 bp, 1018 bp, and 517 bp shown in bold.

In the contaminated column, the presence of prominent PCR products at 690 bp and 594 bp found throughout the column during the first 4 months suggests that the microbial community had quickly adapted after one month due to the petroleum contamination (Fig 11A). Additionally, from the second sampling month through 20

months, bacteria represented by the PCR products at 921 bp and 883 bp appear to migrate downward through the column. These results suggest that the microbial community is continually changing throughout the entire sampling period. In contrast, the control column shows an even microbial distribution throughout the vertical sampling in the column (Fig. 11B). The lanes do not contain many prominent PCR products, but rather a variety of PCR products of different sizes, indicative of a highly variable intergenic spacer region from a diverse community of microbes. There was a slight alteration in the microbial community structure from the first month to the second month as the microbial community adapted to the column; however, in subsequent months the RISA profiles show little change. The 20 month sample does show some perturbation in the community at sample depths below 25 cm with the emergence of several distinct PCR products found in samples from above the water table. Overall, these results suggest that the contaminated column contained a highly perturbed microbial community adapting over time, while the uncontaminated column experienced fewer changes and maintained a greater diversity throughout the experiment.

16S rRNA Gene Sequencing and Phylogenetic Analysis

While RISA profiles allow for the observation of overall changes in the microbial community structure quickly and easily, they are not able to characterize specific microbial populations from within the different environments. Alternative approaches using 16S rRNA gene cloning and sequencing provide a powerful tool for the identification of specific populations within the microbial community. Therefore,

16S rRNA gene libraries were constructed from sediment samples collected within the free phase petroleum zone of the contaminated column where the greatest increase in conductivity occurred, and the respective depth in the control column. A total of four 16S rRNA gene libraries were constructed from samples collected in the second and twentieth month at the 45 cm depth in each of the columns.

The two libraries constructed from the 2 month sampling date from the control column VRC6 (ES6) and contaminated column VRC7 (ES7), contained 86 and 91 clones, respectively, while the two libraries from the 20 month sampling date, JA6 (control) and JA7 (contaminated), contained 80 and 86 clones with 16S rRNA gene inserts, respectively (Table 4).

Table 4

Summary of the 16S rRNA Gene Libraries from the Laboratory Columns

Column	Sampling month	Total # of clones	# of clones sequenced	Shannon Wiener index	
				H'	*J*
Contaminated	2	91	48	1.80	0.68
	20	86	55	2.23	0.79
Control	2	86	50	2.04	0.72
	20	80	51	2.27	0.82

16S rRNA gene inserts were PCR amplified and digested with restriction endonucleases *Msp*I. Groups of clones with identical restriction fragment length polymorphism (RFLP) patterns were ranked in order of abundance, and Shannon-Wiener diversity indices were calculated. The diversity of the two libraries was reflected in their Shannon-Wiener diversity index (*H'*) and Shannon equitability value (*J*) (Table 4). The uncontaminated column had greater diversity and equitability values (H=2.04, J=0.72) than the contaminated column (H=1.80, J=0.68) in the

second month, demonstrating the effect of petroleum contamination to select for microbial populations which can survive in the perturbed environment. However, in both the contaminated and control column, the diversity of the both communities increased over time to similar *H* values of 2.27 (control) and 2.23 (contaminated), suggesting that adaptation of the microbial community to the laboratory conditions occurred over time. It is interesting to note that Shannon-Wiener diversity and equitability values from the field (Table 1) were much higher than from the columns, reflecting the bias which occurs in the laboratory for those microorganisms that are able to adapt to the lab conditions.

All unique clones as determined by RFLP plus a single representative clone from the identical RFLP groups were used for DNA sequencing and phylogenetic analysis. Clones with over 98% sequence identity were grouped together as operational taxanomic units (OTUs). Phylogenetic analysis of 16S rDNA sequences revealed a diverse microbial community associated with sediments from the both laboratory columns for all time points. Table 5 shows the percent composition by phylogenetic class for each of the 16S rRNA gene libraries, which are represented by pie charts in Figure 12. In the second month, the *Actinobacteria* were the largest population within both the contaminated (55%) and control (37%) columns. Within the *Actinobacteria*, the most abundant sequences detected in both columns shared over 99% sequence identity to *Rhodococcus erythropolis* (Table 6). *Rhodococcus* are common soil microbes, with diverse metabolic capabilities including degradation of a wide range of aliphatic and aromatic hydrocarbons (Kim *et al.*, 2002). The remaining portion of *Actinobacteria* detected in the contaminant column was affiliated with *Mycobacterium rhodeiae* (99% identity; Table 6). As *Rhodococcus*, *Mycobacterium* contains a wide array of genes coding for enzymes used in the degradation of many

contaminant compounds including alkanes, polycyclic aromatic hydrocarbons (PAH), and vinyl chlorides (Cheung & Kinkle, 2001; Churchill *et al.*, 1999). However, both of these populations were not detected in either of the columns at the later 20 month sampling date (Table 6).

Table 5

Microbial Composition of 16S rRNA Gene Libraries from the Laboratory Columns

Phylogenetic Class	Percent composition			
	Contaminated		Control	
	2	20	2	20
Actinobacteria	61	5	43	-
Alphaproteobacteria	4	9	35	26
Bacilli	25	28	12	47
Bacteroidetes	2	31	3	5
Planctomycetes	-	-	3	6
Betaproteobacteria	3	2	2	8
Gammapoteobacteria	-	1	1	1
Deltaproteobacteria	-	5	1	-
Gemmatimonadetes	1	1	-	1
WS6	-	-	-	6
Clostridia	2	13	-	-
Spirochaetes	-	5	-	-
Verrucomicrobia	1	-	-	-
Green nonsulfur	1	-	-	-

A significant enrichment of several *Bacillus* species was detected in each of the columns for both sampling dates. The largest population shared 99% sequence identity to *Bacillus drentensis* originally isolated from agricultural soils (Heyrman *et al.*, 2004). Members of the genus *Bacillus* are widespread in the environment, and can adapt to a wide array of environmental conditions, which may be in part due to their ability to produce endospores (Madigan *et al.*, 2003). *Bacillus* species are also

easily cultured in the lab using standard media, and their presence in all samples reflects this trait.

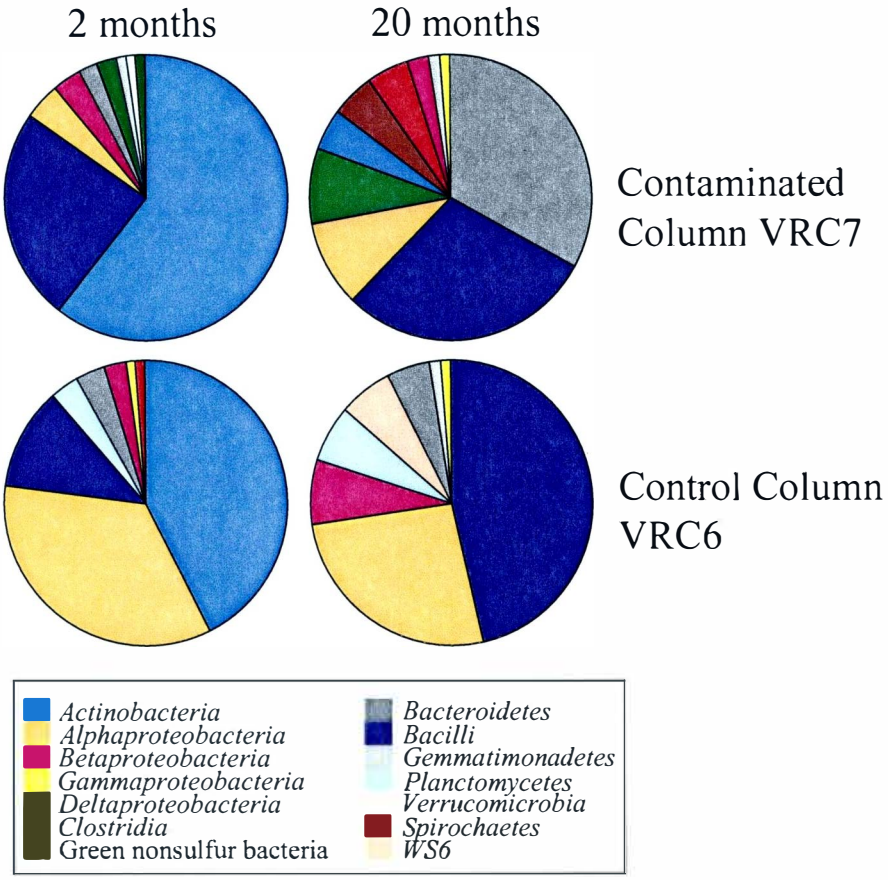

Figure 12. Microbial Community Composition of Laboratory Columns. The microbial community composition was determined by 16S rRNA gene sequencing. Pie charts show the different microbial populations by divisions for the contaminated and control columns at the 2nd and 20th sampling dates.

There were also several populations detected only in the contaminated column sediments. Populations with relation of *Bacteroidetes* clone AKYG450 were detected in low amounts in the contaminated column at both the 2 and 20 month sampling

dates, but the most abundant *Bacteroidetes* clone RsW01039 (26 replicates) was detected only in the 20th month (Table 6). Overall, the proportion of *Bacteroidetes* increased from 2% to 27% by 20 months (Table 5). Populations with affiliation to *Clostridium acidisoli* were also detected at both sampling dates within the contaminated column (Table 6). The number of clones with high identity to *Clostridium acidisoli* increased from one clone in the 2nd month to 6 clones in the 20th month, demonstrating a slight increase the proportion of *Clostridia* in the contaminated sediments. An additional *Clostridia* population with affiliation to *Sedimentibacter* sp. C7 was detected only in the contaminated column after 20 months. There was also a small population (4 clones) of *Spirochaetes* with over 99% identity to the WCHB14 uncultured eubacterium clone detected in petroleum contaminated sediments at the Wurtsmith Airforce base study site (Dojka *et al.*, 1998). Populations of *Clostridia*, *Bacteroidetes*, and *Spirochaetes* are commonly found in anaerobic petroleum contaminated sediments and have a fermentative, or acetogenic metabolism (Feris *et al.*, 2004; Leadbetter *et al.*, 1999; Soucaille & Goma, 1986).

In contrast to clones detected in the contaminated column only, many of the other clones were detected only in the control column. These included several populations commonly isolated from various soils with high sequence identity to *Sphingomonas asaccharolytica*, *Mesorhizobium alexandrii*, *Kaistia* sp. BBTR58, *Devosia riboflavina*, and *Rhodanobacter* sp. CHNTR45 from within the α-, β, and γ-*Proteobacteria* subdivisions, *Pirellula staleyi* and *Gemmata obscuriglobus* from within the *Planctomycetes*, as well as an uncultured clone clustering within the candidate WS6 division (Table 6).

In order to determine if the microbial community composition for each of the

columns at each time point was significantly different, the Libshuff program was used (Singleton *et al.*, 2001). Libshuff calculated *p*-values of less than 0.05 are considered to be an indicator of significant difference. For the four libraries from the contaminated and uncontaminated locations, Libshuff pairwise comparisons revealed significant differences among all libraries with calculated *p*-values < 0.001. These results demonstrate that the microbial communities from each of the columns reflect the different and changing environmental conditions, and suggest that as observed in similar field studies, the observed geophysical changes over time in petroleum contaminated sediments may be due to the microbial activity of distinct populations within those electrically conductive zones.

Table 6

Sequence Type Distribution for the Laboratory Columns

Representative clone	# of clones within each library				Phylogenetic division	Nearest neighbor (accession no.)	% Similarity
	VRC7		VRC6				
	2mo	20mo	2mo	20mo			
ES743	1				Green nonsulfur	*Sphaerobacter thermophilus* (AJ420142)	93
JA611				5	WS6	WS6 clone 072DZ58 (DQ397487)	94
JA736		4			Spirochetes	WCHB14 uncultured bacterium (AF050549)	99
ES680, JA647			14	2	*Alphaproteobacteria*	*Sphingomonas asaccharolytica* (AJ871435)	95
ES638, JA743, JA622		5	1	2	*Alphaproteobacteria*	*Brevundimonas* sp. TibetIX23 (DQ177489)	99
ES659, JA737		1	3		*Alphaproteobacteria*	*Caulobacter* sp. H62 (AB076664)	99
ES734	1				*Alphaproteobacteria*	*Beijerinckia indica* (AB119199)	96
JA738		1			*Alphaproteobacteria*	*Bosea thiooxidans* (AJ250798)	99
ES747	1				*Alphaproteobacteria*	*Bradyrhizobium liaoningense* (DQ497619)	98
ES619, JA618, ES717, JA782	2	1	2	14	*Alphaproteobacteria*	*Afipia felis* (AY548800)	100
ES665, JA623			1	3	*Alphaproteobacteria*	*Mesorhizobium alexandrii* (AJ786600)	94
ES648			3		*Alphaproteobacteria*	*Kaistia* sp. BBTR58 (DQ337585)	99
ES62			6		*Alphaproteobacteria*	*Devosia riboflavina* (AF501346)	99
ES784	2				*Betaproteobacteria*	*Variovorax* sp. WDL1 (AF538929)	98
JA691, JA739		2		2	*Betaproteobacteria*	*Alcaligenes* sp. R21939 (AJ786800)	97
ES632			1		*Betaproteobacteria*	*Rhodanobacter* sp. CHNTR45 (DQ337598)	96
ES643, ES773, JA632	1		1	4	*Betaproteobacteria*	*Herbaspirillum frisingense* (AY043372)	97
ES68			1		*Gammaproteobacteria*	*Methylobacter* sp. LW1(AF150784)	98

Table 6 cont…

Representative clone	# of clones within each library				Phylogenetic division	Nearest neighbor (accession no.)	% Similarity
	VRC7		VRC6				
	2mo	20mo	2mo	20mo			
JA689, JA799		1		1	*Gammaproteobacteria*	*Lysobacter* sp. Dae08 (AB249682)	97
JA747		4			*Deltaproteobacteria*	*Deltaproteobacterium* clone (AY921889)	95
ES635			1		*Deltaproteobacteria*	*Bdellovibrio* sp. L (Y294214)	97
ES753, JA746	1	1			*Gemmatimonadetes*	Uncultured clone KD666 (AY218764)	95
JA671				1	*Gemmatimonadetes*	Uncultured clone AKYH1347 (AY921725)	99
JA66				3	*Bacteroidetes*	*Bacteroidetes* clone IRD18D05 (AY947931)	96
JA657				1	*Bacteroidetes*	Uncultured clone KD857 (AY218692)	98
ES770, JA716	2	1			*Bacteroidetes*	*Bacteroidetes* clone AKYG450 (AY922017)	96
JA789		26			*Bacteroidetes*	*Bacteroidales* clone RsW01039 (AB198473)	97
ES61			3		*Bacteroidetes*	*Pedobacter africanus* (AJ438171)	98
ES72	27				*Actinobacteria*	*Mycobacterium rhodesiae* (AJ429047)	99
ES69, ES71	28		35		*Actinobacteria*	*Rhodococcus erythropolis* (AF501339)	99
ES675, JA785		4	1		*Actinobacteria*	*Arthrobacter* sp AG1 (AY651317)	99
JA740, ES767	1	6			*Clostridia*	*Clostridium acidisoli* (AJ23775)	99
JA732		5			*Clostridia*	*Sedimentibacter* sp C7(AY76646)	98
ES795, JA787, JA644	1	1		3	*Bacilli*	*Oxalophagus oxalicus* (Y14581)	96
JA793		4			*Bacilli*	*Paenibacillus favisporus* (AY308758)	98
JA652				3	*Bacilli*	*Bacillus ehimensis* (AY116666)	99
JA679				5	*Bacilli*	*Bacillus benzoevorans* (DQ29811)	99
ES778, JA685, JA778, ES610	22	19	10	26	*Bacilli*	*Bacillus drentensis* (DQ275176)	99
JA649, ES684			1	5	*Planctomycetes*	*Pirellula staleyi* ATCC 35122 (AF399914)	99
ES625			2		*Planctomycetes*	*Gemmata obscuriglobus* (X81957)	96
ES716	1				*Verrucomicrobia*	*Verrucomicrobium* DEV031 (AJ401123)	91

Discussion

In the field study (Chapter III), analysis a subsurface petroleum plume revealed complex biogeophysical relationships which exist in the petroleum contaminated sediments. Changes in the microbial community structure at these sites were found to be concomitant with altered geophysical signatures. Therefore, laboratory columns were constructed to simulate petroleum contaminated and background conditions in order to study the spatial and temporal biogeophysical relationships of petroleum contaminated sediments. Both culture-dependent and culture-independent microbial analyses were performed to provide evidence that bioremediation was occurring, and to demonstrate that changes in the geophysical properties of the contaminated sediments were due to microbial activity.

The highest numbers of hydrocarbon degrading microbes were recorded in the contaminated column by the second month in the free phase contaminant zone and in the upper sediments in subsequent sampling periods, demonstrating a rapid adaptation by the microbial community to the petroleum contaminant as well as a long-term persistence over the entire experiment (Fig 9). The results from the contaminated column contrasted with those recorded in the control column where the number of hydrocarbon degrading bacteria remained significantly low (Fig. 10). Culture-based techniques are commonly used as an indicator for microbial biodegradation of contaminant compounds (Haack & Bekins, 2000), and thus the increase in hydrocarbon degrading microbes in the contaminated column provides support that biodegradation of the hydrocarbons from the diesel contaminant occurred throughout the experiment.

Culture dependent methods are known to have limitations because so few

environmental microorganisms are able to grow in laboratory cultures (Pace, 1997; Rappe & Giovannoni, 2003). Therefore, culture independent RISA analysis was performed to determine any changes in the overall microbial community structure, either spatially within the column or temporally over the entire experiment. The RISA results reflect early changes in the microbial community composition (Fig. 11A). Large changes in the RISA profile of the contaminated column occurring between the first and second sampling periods in the free phase contaminant zone (45 cm), specifically the emergence of the 594 bp and 690 bp PCR products, are most likely reflective of the large increase in hydrocarbon-degrading microbes detected by MPN analysis from the same depth. Further changes in the microbial community structure were visible at the subsequent 12 and 20 month sampling dates. The loss of the 594 bp and 690 bp PCR products at the 45 cm depth could reflect the decrease in hydrocarbon degrading numbers in the lower depths. The higher number of hydrocarbon degraders observed in the upper depths from the MPN analysis (Fig. 9) observed in the 12^{th} and 20^{th} month were not consistent with the RISA profiles. This could reflect the biased selection of microbes which can be cultured in the lab, and not their relative abundance in the community. However, the large population of hydrocarbon degrading microbes from the 20^{th} sampling period from the 35 cm depth coincides with the location in which the largest change in electrical conductivity occurred, suggesting that these populations could play a role in altering the sediment geophysical properties. In contrast to the contaminated column, the control column showed less variability in the RISA profiles between sampling dates, indicating increased diversity and temporal stability in the microbial community over the course of the entire experiment (Fig. 11B). This was reflected in the low conductivity values of the control column observed throughout the course of the experiment.

Comparison of the microbial data with the geoelectrical data from the contaminated column reveals a possible link between microbial activity and subsurface geophysical properties. As observed in the MPN and RISA results, changes in the microbial community structure and a large increase in the amount of hydrocarbon degrading microbes occurred by the 2nd month (Fig. 9, Fig. 11A). This community maintained relative stability over the next two months as seen in the RISA profile for the 4th month (Fig 11). Following an initial equilibration period, the electrical conductivity of the contaminated column began to increase in the petroleum impacted zone by the 4th month (Fig. 7C). As the microbial community began to change (demonstrated by RISA profiles in month 2 and 12) the electrical conductivity in the contaminated sediments began to continually increase through the end of the experiment. Therefore it appears that a change in the microbial community structure preceded a change in the electrical conductivity of the sediments, and that further changes in community structure resulted in a continued increase in electrical conductivity. Thus, we suggest that the changes in the geophysical properties of petroleum contaminated sediments from resistive to conductive were a result of microbial activity.

To characterize the microbial populations whose activity seems to play a role in increasing the subsurface conductivity and to elucidate the microbial processes which alter the biogeophysical properties of petroleum contaminated sediments, 16S rRNA gene libraries were constructed from sediments collected before and after the conductivity change. The microbial communities before the conductivity change were composed mainly of aerobic hydrocarbon degraders including populations of *Rhodococcus* and *Mycobacterium* (Table 6) (Cheung & Kinkle, 2001; Churchill *et al.*, 1999; Kim *et al.*, 2002). The control column also had a large population of

Rhodococcus. This is not surprising because rhodococci are found as common members of soil microbial communities, and have been easily cultured on standard laboratory media from sediments collected from the contaminated Carson City site (Duris, 2002). Comparison of the microbial community from the 2nd month to that of the 20th month, after the conductivity change, showed a shift from an aerobic community to an anaerobic community, composed largely of anaerobic hydrocarbon degrading such as *Brevundimonas*, *Clostridium acidisoli*, and *Sedimentibacter*, as well as acetogens such as *Bacteroidetes*, and *Spirochaetes* uncultured clones .

Fermenting anaerobic organisms tend to produce high amounts of organic acids as a byproduct of hydrocarbon degradation (Cozzarelli *et al.*, 1990; Cozzarelli *et al.*, 1994). As shown in field studies, an increase in organic acid production drives mineral dissolution and the release of ions such as Ca^+ into the pore water (Bennett & Melcer, 1988). Analysis of the pore water in the contaminated column had shown an increase in Ca^+ levels (Sherrod, 2003). As described in Chapter III from the field site, the changes in electrical conductivity were not due to sediment lithology (the sediment type was uniform throughout the column, as well as the fluid saturation), supporting the previous suggestion that increases in electrical conductivity of petroleum contaminated sediments were due to either changes in the fluid electrolytic properties or changes in the interfacial grain surface properties. In fact, SEM images of the sediment grains from the contaminated column did show changes to the grain interfacial properties including extensive biofilm coverage and mineral precipitation (Estella Atekwana, unpublished observations).

The presence of acetogenic and not methanogenic communities in the contaminated column also demonstrates the artificial environment provided by the laboratory columns, which selects for microbial populations that can adapt to the

laboratory conditions. Additionally, the large *Bacillus* populations in both the contaminated and control columns reflect their ability to survive in a wide range of environments and their amenability to laboratory settings (Madigan *et al.*, 2003). It is interesting to note that even in the artificial laboratory environment, similar changes in the geophysical properties of the contaminated sediments as compared to contaminated field studies were observed. This suggests that even though different microbial populations exist in the laboratory experiments, that similar microbial processes are occurring under anaerobic conditions, which alter the subsurface to a degree that is detectable using geophysical methodologies.

In conclusion, we have demonstrated that spatial and temporal changes in the microbial community structure of hydrocarbon contaminated sediments result in an alteration in the geophysical properties of the contaminated subsurface detectable by an increase in the bulk conductivity of the sediments. The low conductivity readings of the background sediments were concomitant with a diverse microbial community with known subsurface microbiota including various *Proteobacteria* and *Planctomycetes*. In fact *Planctomycetes* appear to be commonly found in uncontaminated sediments and may be a useful biomarker in determining the absence of hydrocarbon contamination (Fuerst, 2004). Conversely, the microbial community found in the electrically conductive petroleum contaminated sediments was consistent with that of aged communities found in other petroleum contaminated sites including aromatic hydrocarbon degrading fermenting organisms (e.g. *Clostridium*), and acetogenic bacteria (e.g. *Spirochaetes*). We speculate that the anomalous increase in electrical conductivity detected in the contaminated laboratory column was attributable to microbial alteration of their environment due to the activity of the anaerobic microbial populations under the anoxic, carbon- and electron donor-rich

environmental conditions.

CHAPTER V

CONCLUSIONS AND OUTLOOK

This study shows the complexity of biogeophysical relationships that exist in the contaminated subsurface. We have demonstrated in field studies that significant changes occur over a vertical gradient in the microbial community structure which parallel changes in LNAPL contamination and subsurface electrical conductivity. We have also shown in laboratory experiments that temporal changes in the microbial community structure precede changes in sediment geophysical properties. The use of culture-independent 16S rRNA gene sequencing allowed for characterization of microbial populations in order to infer their metabolic capabilities and environmental interactions at the biophysicochemical level, as well as the ways in which microorganisms modify and respond to changes in their environment.

Based on these results and comparison to other studies, we can begin to summarize the microbiological impact on geophysical properties of the contaminated subsurface. Figure 13 shows a schematic diagram depicting the biogeophysical relationships of petroleum contaminated sediments based on a modified model from Abdel Aal *et al.* (2004). Upon initial subsurface contamination, the LNAPL displaces groundwater in the pore space and partitions in to residual, dissolved, and free product phases. The electrical properties of freshly contaminated sediments remain highly resistive (low conductance) due to the insulating properties of the hydrocarbons (DeRyck *et al.*, 1993). In a freshly contaminated aquifer, petroleum

hydrocarbons provide a readily available carbon source to stimulate the initial aerobic microbial degradation. This consumes any available oxygen, rapidly driving the system anoxic. In the anoxic state a stepwise utilization of terminal electron acceptors occurs based on the greatest potential energy including nitrates, ferric iron, sulfates, and finally methanogenesis or acetogenesis (Chapelle & Bradley, 1997). Within the aged petroleum contaminated aquifer at the field site, as well as the contaminated laboratory column after 20 months, a low availability of alternative TEAs resulted in large methanogenic and acetogenic bacterial populations as well as a significant proportion of hydrocarbon degrading fermenting microbes. As seen in other aged petroleum contaminated sites, hydrocarbon degrading fermenting organisms begin to produce large amounts of organic acids, which results in mineral dissolution of the surrounding sediment grains (Cozzarelli *et al.*, 1990). Mineral dissolution releases cations such as Ca^{2+} into the pore fluid, increasing the ionic strength of the solution (Bennett & Melcer, 1988; Bennett, 1991; Bennett *et al.*, 1996; Sauck, 2000). An increase in fluid ionic strength results in an increase in electrical conductance through the fluid, and has been demonstrated to promote microbial attachment (Roberts *et al.*, 2004; Zita & Hemansoon, 1994). As microbes attach to the grain surface and form biofilm communities, there is an increase in sediment grain surface area, cations become trapped at the fluid-surface interface (Geddie & Sutherland, 1993; Hersman *et al.*, 1996), and conductive metal sulfides precipitate out from the activity of DIRB and SRB, effectively altering the interfacial properties of the sediment grains (Ntarlagiannis *et al.*, 2005; Williams *et al.*, 2005). Changes to the interfacial properties of the sediment grains enhance electrical conduction through the

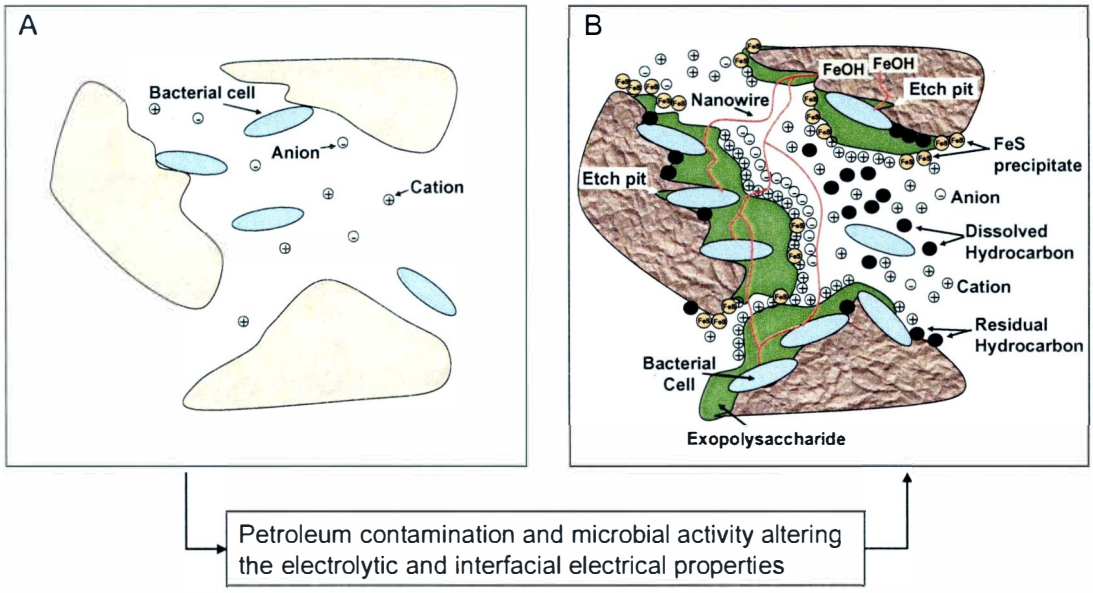

Figure 13. Schematic Drawing to Model the Biogeophysical Changes Occurring Within Aged Petroleum Contaminated Sediments. (A) Uncontaminated sediments containing low levels of ions in solution will have dispersed and attached bacteria and low electrical conductivity. (B) Petroleum contamination stimulates microbial activity. Alteration in the electrical properties of the contaminated sediments begins with mineral dissolution by organic acids produced from hydrocarbon biodegradation. This results in an increase in ionic concentration, which in turn promotes further microbial attachment. Changes in the sediment interfacial properties result from microbial attachment, biofilm formation and trapping of cations, and precipitation of metal sulfides on to sediment surfaces. Furthermore microbial nanowires used for electron transfer during anaerobic respiration may also alter the geophysical properties. The combined electrolytic and interfacial changes result in an increased electrical conductivity in the petroleum contaminated zone.

naturally resistive media. Additionally, although not specifically tested for in this work, the recent discovery of biological nanowires (electrically conductive appendages) produced by DIRB such as *Geobacter*, *Shewanella*, and *Pelotomaculum* under carbon rich, electron acceptor limiting conditions, suggests that the presence of nanowires may also have an impact on electrical conductance in the subsurface (Lies *et al.*, 2005; Reguera *et al.*, 2005).

Because microorganisms have the ability to effectively alter the geophysical properties of their environment through their metabolic activity, geophysical methods are able to isolate zones where these activities are elevated due to the abundance of a carbon source (petroleum). Traditionally, geochemical methods have been used to determine the disappearance of contaminant mass, but geochemical analysis is restricted to the water saturated zone. Therefore, we suggest that the combination of both microbiological and geophysical techniques will provide a powerful tool to monitor the bioremediation of petroleum contaminated sediments.

APPENDIX

GENBANK ACCESSION NUMBERS

5V	Accession	5F	Accession	5C	Accession	5S	Accession
5V1	DQ663791	5F26	DQ663861	5C1	DQ663929	5S1	DQ663993
5V2	DQ663792	5F27	DQ663862	5C2	DQ663930	5S2	DQ663994
5V3	DQ663793	5F29	DQ663863	5C3	DQ663931	5S3	DQ663995
5V4	DQ663794	5F30	DQ663864	5C4	DQ663932	5S4	DQ663996
5V5	DQ663795	5F31	DQ663865	5C5	DQ663933	5S5	DQ663997
5V6	DQ663796	5F34	DQ663866	5C6	DQ663934	5S7	DQ663998
5V7	DQ663797	5F35	DQ663867	5C8	DQ663935	5S8	DQ663999
5V8	DQ663798	5F36	DQ663868	5C9	DQ663936	5S10	DQ664000
5V9	DQ663799	5F37	DQ663869	5C12	DQ663937	5S11	DQ664001
5V10	DQ663800	5F38	DQ663870	5C13	DQ663938	5S12	DQ664002
5V12	DQ663801	5F40	DQ663871	5C14	DQ663939	5S13	DQ664003
5V13	DQ663802	5F44	DQ663872	5C17	DQ663940	5S15	DQ664004
5V15	DQ663803	5F46	DQ663873	5C18	DQ663941	5S16	DQ664005
5V16	DQ663804	5F47	DQ663874	5C19	DQ663942	5S17	DQ664006
5V17	DQ663805	5F48	DQ663875	5C20	DQ663943	5S18	DQ664007
5V18	DQ663806	5F49	DQ663876	5C21	DQ663944	5S25	DQ664008
5V19	DQ663807	5F50	DQ663877	5C22	DQ663945	5S26	DQ664009
5V20	DQ663808	5F51	DQ663878	5C24	DQ663946	5S27	DQ664010
5V21	DQ663809	5F52	DQ663879	5C25	DQ663947	5S29	DQ664011
5V22	DQ663810	5F54	DQ663880	5C26	DQ663948	5S31	DQ664012
5V23	DQ663811	5F58	DQ663881	5C28	DQ663949	5S32	DQ664013
5V24	DQ663812	5F59	DQ663882	5C29	DQ663950	5S33	DQ664014
5V25	DQ663813	5F60	DQ663883	5C31	DQ663951	5S35	DQ664015
5V26	DQ663814	5F61	DQ663884	5C32	DQ663952	5S41	DQ664016
5V30	DQ663815	5F62	DQ663885	5C34	DQ663953	5S42	DQ664017
5V31	DQ663816	5F64	DQ663886	5C35	DQ663954	5S43	DQ664018
5V33	DQ663817	5F65	DQ663887	5C36	DQ663955	5S44	DQ664019
5V34	DQ663818	5F66	DQ663888	5C37	DQ663956	5S45	DQ664020
5V35	DQ663819	5F67	DQ663889	5C38	DQ663957	5S49	DQ664021
5V36	DQ663820	5F68	DQ663890	5C39	DQ663958	5S50	DQ664022
5V39	DQ663821	5F69	DQ663891	5C40	DQ663959	5S54	DQ664023
5V42	DQ663822	5F71	DQ663892	5C43	DQ663960	5S60	DQ664024
5V43	DQ663823	5F72	DQ663893	5C44	DQ663961	5S61	DQ664025
5V44	DQ663824	5F74	DQ663894	5C47	DQ663962	5S62	DQ664026

5V45	DQ663825	5F75	DQ663895	5C48	DQ663963	5S65	DQ664027
5V46	DQ663826	5F76	DQ663896	5C49	DQ663964	5S66	DQ664028
5V47	DQ663827	5F77	DQ663897	5C52	DQ663965	5S69	DQ664029
5V48	DQ663828	5F78	DQ663898	5C53	DQ663966	5S71	DQ664030
5V49	DQ663829	5F79	DQ663899	5C54	DQ663967	5S74	DQ664031
5V50	DQ663830	5F80	DQ663900	5C55	DQ663968	5S75	DQ664032
5V52	DQ663831	5F81	DQ663901	5C58	DQ663969	5S76	DQ664033
5V53	DQ663832	5F82	DQ663902	5C59	DQ663970	5S78	DQ664034
5V54	DQ663833	5F83	DQ663903	5C62	DQ663971	5S84	DQ664035
5V55	DQ663834	5F84	DQ663904	5C63	DQ663972	5S85	DQ664036
5V57	DQ663835	5F86	DQ663905	5C64	DQ663973	5S88	DQ664037
5V58	DQ663836	5F87	DQ663906	5C66	DQ663974	5S89	DQ664038
5V60	DQ663837	5F88	DQ663907	5C68	DQ663975	5S91	DQ664039
5V61	DQ663838	5F89	DQ663908	5C70	DQ663976	5S93	DQ664040
5V62	DQ663839	5F90	DQ663909	5C72	DQ663977	5S94	DQ664041
5V63	DQ663840	5F92	DQ663910	5C73	DQ663978	5S96	DQ664042
5V64	DQ663841	5F93	DQ663911	5C75	DQ663979		
5V66	DQ663842	5F94	DQ663912	5C77	DQ663980		
5V67	DQ663843	5F95	DQ663913	5C78	DQ663981		
5V68	DQ663844	5F96	DQ663914	5C79	DQ663982		
5V69	DQ663845	5F97	DQ663915	5C80	DQ663983		
5V74	DQ663846	5F98	DQ663916	5C83	DQ663984		
5V76	DQ663847	5F99	DQ663917	5C84	DQ663985		
5V78	DQ663848	5F100	DQ663918	5C86	DQ663986		
5V79	DQ663849	5F101	DQ663919	5C88	DQ663987		
5V81	DQ663850	5F102	DQ663920	5C89	DQ663988		
5V82	DQ663851	5F104	DQ663921	5C90	DQ663989		
5V83	DQ663852	5F105	DQ663922	5C92	DQ663990		
5V84	DQ663853	5F106	DQ663923	5C94	DQ663991		
5V87	DQ663854	5F108	DQ663924	5C95	DQ663992		
5V88	DQ663855	5F110	DQ663925				
5V89	DQ663856	5F112	DQ663926				
5V90	DQ663857	5F113	DQ663927				
5V91	DQ663858	5F114	DQ663928				
5V92	DQ663859						
5V95	DQ663860						

9V	Accession	9S	Accession
9V5	DQ664043	9S2	DQ664108
9V6	DQ664044	9S3	DQ664109
9V7	DQ664045	9S4	DQ664110
9V10	DQ664046	9S5	DQ664111
9V12	DQ664047	9S6	DQ664112
9V14	DQ664048	9S7	DQ664113
9V15	DQ664049	9S8	DQ664114
9V16	DQ664050	9S10	DQ664115
9V19	DQ664051	9S11	DQ664116
9V21	DQ664052	9S13	DQ664117
9V23	DQ664053	9S15	DQ664118
9V24	DQ664054	9S16	DQ664119
9V25	DQ664055	9S17	DQ664120
9V26	DQ664056	9S18	DQ664121
9V29	DQ664057	9S19	DQ664122
9V30	DQ664058	9S20	DQ664123
9V31	DQ664059	9S21	DQ664124
9V32	DQ664060	9S22	DQ664125
9V33	DQ664061	9S23	DQ664126
9V34	DQ664062	9S25	DQ664127
9V35	DQ664063	9S26	DQ664128
9V37	DQ664064	9S31	DQ664129
9V38	DQ664065	9S33	DQ664130
9V39	DQ664066	9S34	DQ664131
9V40	DQ664067	9S35	DQ664132
9V41	DQ664068	9S36	DQ664133
9V42	DQ664069	9S38	DQ664134
9V43	DQ664070	9S39	DQ664135
9V44	DQ664071	9S40	DQ664136
9V45	DQ664072	9S42	DQ664137
9V46	DQ664073	9S43	DQ664138
9V49	DQ664074	9S44	DQ664139
9V50	DQ664075	9S45	DQ664140
9V51	DQ664076	9S47	DQ664141
9V52	DQ664077	9S48	DQ664142
9V54	DQ664078	9S50	DQ664143
9V57	DQ664079	9S51	DQ664144
9V58	DQ664080	9S53	DQ664145
9V59	DQ664081	9S54	DQ664146
9V61	DQ664082	9S55	DQ664147
9V62	DQ664083	9S56	DQ664148

9V63	DQ664084	9S57	DQ664149
9V66	DQ664085	9S58	DQ664150
9V69	DQ664086	9S59	DQ664151
9V71	DQ664087	9S60	DQ664152
9V72	DQ664088	9S61	DQ664153
9V73	DQ664089	9S62	DQ664154
9V74	DQ664090	9S63	DQ564155
9V75	DQ664091	9S64	DQ664156
9V76	DQ664092	9S68	DQ664157
9V77	DQ664093	9S69	DQ664158
9V78	DQ664094	9S70	DQ664159
9V79	DQ664095	9S73	DQ664160
9V80	DQ664096	9S74	DQ664161
9V81	DQ664097	9S75	DQ664162
9V83	DQ664098	9S76	DQ664163
9V85	DQ664099	9S78	DQ664164
9V86	DQ664100	9S79	DQ664165
9V87	DQ664101	9S80	DQ664166
9V90	DQ664102	9S81	DQ664167
9V91	DQ664103	9S82	DQ664168
9V93	DQ664104	9S84	DQ664169
9V94	DQ664105	9S85	DQ664170
9V95	DQ664106	9S86	DQ664171
9V97	DQ664107	9S87	DQ664172
		9S88	DQ664173
		9S89	DQ664174
		9S90	DQ664175
		9S91	DQ664176
		9S94	DQ664177
		9S95	DQ664178
		9S96	DQ664179

BIBLIOGRAPHY

Abdel Aal, G. Z., Atekwana, E. A., Slater, L. D. & Atekwana, E. A. (2004). Effects of microbial processes on electrolytic and interfacial electrical properties of unconsolidated sediments. *Geophys Res Lett* **31**, L12505.

Altschul, S. F., Gish, W., Miller, W., Myers, E. W. & Lipman, D. J. (1990). Basic local alignment search tool. *J Mol Biol* **215**, 403-410.

Archie, G. E. (1942). The electrical resistivity log as an aid in determining some reservoir characteristics. *Trans Am Inst Min Metall Pet Eng* **146**, 54-62.

Atekwana, E. A., Sauk, W. A. & Werkema, D. D. (2000). Investigations of geoelectrical signatures at a hydrocarbon contaminated site. *J Appl Geophys* **44**, 167-180.

Atekwana, E. A., Atekwana, E. A., Rowe, R. S., Werkema, D. D. & Legall, F. D. (2004a). The relationship of total dissolved solids measurements to bulk electrical conductivity in an aquifer contaminated with hydrocarbon. *J Appl Geophysics* **56**, 281-294.

Atekwana, E. A., Atekwana, E. A., Werkema, D. D., Allen, J. P., Smart, L. A., Duris, J. W., Cassidy, D. P., Sauck, W. A. & Rossbach, S. (2004b). Evidence for microbial enhanced electrical conductivity in hydrocarbon-contaminated sediments. *Geophys Res Lett* **31**, 1-4.

Atekwana, E. A., Atekwana, E. A., Legall, F. D. & Krishnamurthy, R. V. (2005). Biodegradation and mineral weathering controls on bulk electrical conductivity in a shallow hydrocarbon contaminated aquifer. *J Contam Hydrol* **80**, 149-167.

Atekwana, E. A., Atekwana, E.A., Werkema, D., Duris, J., Rossbach, S., Sauk, W., Koretsky, C., Cassidy, D., Means, J., Sherrod, L. (2003). Investigating the effects of microbial communities on electrical properties of soils: Preliminary results from a pilot scale column experiment. *Geophys Res Abstr* **5**, 13,832.

Atlas, R. M. (1995). Petroleum biodegradation and oil spill bioremediation. *Mar Pollut Bull* **31**, 178-182.

Atlas, R. M. & Bartha, R. (1998). *Microbial Ecology*. Reading, Massachusetts: Benjamin/Cummings Publishing Co.

Banfield, J. F., Welch, S. A., Zhang, H., Ebert, T. T. & Penn, R. L. (2000). Aggregation-based crystal growth and microstructure development in natural iron oxyhydroxide biomineralization products. *Science* **289**, 751-754.

Banning, N., Brock, F., Fry, J. C., Parkes, R. J., Hornibrook, E. R. C. & Weightman, A. J. (2005). Investigation of the methanogen population structure and activity in a brackish lake sediment. *Environ Microbiol* **7**, 947-960.

Barns, S. M., Takala, S. L. & Kuske, C. R. (1999). Wide distribution and diversity of members of the bacterial kingdom *Acidobacterium* in environment. *Applied and Environmental Microbiology* **65**, 1731-1737.

Bennett, P. C. & Melcer, S., Hassett (1988). The dissolution of quartz in dilute aqueous solutions of organic acids at 25 degrees celcius. *Geochim Cosmochim Acta* **52**, 1521-1530.

Bennett, P. C. (1991). The dissolution of quartz in organic-rich aqueous systems. *Geochim Cosmochim Acta* **55**, 1781-1797.

Bennett, P. C., Hiebert, F. K. & Choi, W. J. (1996). Microbial colonization and weathering of silicates in a petroleum-contaminated groundwater. *Chem Geol* **132**, 45-53.

Bennett, P. C., Rogers, J. R., Choi, W. J. & Hiebert, F. K. (2001). Silicates, silicate weathering, and microbial ecology. *Geomicrobiol J* **18**, 3-19.

Bermejo, J. L., Sauck, W. A. & Atekwana, E. A. (1997). Geophysical discovery of a new LNAPL plume at former Wurtsmith AFB, Oscoda, Michigan. *Ground Water Monit Remediat* **17**, 131-137.

Boone, D. R. & Bryant, M. P. (1980). Propionate-degrading bacterium, *Syntrophobacter wolinii* sp. nov. gen. nov., from methanogenic ecosystems. *Appl Environ Microbiol* **40**, 626-632.

Borneman, J. & Triplett, E. W. (1997). Molecular microbial diversity in soils from eastern amazonia: evidence for unusual microorganisms and microbial population shifts associated with deforestation. *Appl Environ Microbiol* **63**, 2647-2653.

Buchholz-Cleven, B. E. E., Rattunde, B. & Straub, K. L. (1997). Screening for genetic diversity of isolates of anaerobic Fe(II)-oxidizing bacteria using DGGE and whole-cell hybridization. *System Appl Microbiol* **20**, 301-309.

Cassidy, D. P., Werkema, D. D., Sauck, W. A., Atekwana, E. A., Rossbach, S. & Duris, J. W. (2001). The effects of LNAPL biodegradation products on electrical conductivity measurements. *J Environ Eng Geophys* **6**, 47-52.

Cassidy, D. P., Hudak, A. J., Werkema, D. D., Atekwana, E. A., Rossbach, S., Duris, J. W., Atekwana, E. A. & Sauck, W. A. (2002). In situ rhamnolipid production at an abandoned petroleum refinery. *Soil Sediment Contam* **11**, 769-787.

Chapelle, F. H. & Bradley, P. M. (1997). Alteration of aquifer geochemistry by microorganisms. In *Manual of Environmental Microbiology*, pp. 558-564. Edited by C. J. Hurst, G. R. Knudsen, M. J. McInerney, L. D. Stetzenbach & M. V. Walter. Washington, D. C.: ASM Press.

Cheung, P. & Kinkle, B. K. (2001). *Mycobacterium* diversity and pyrene mineralization in petroleum-contaminated soils. *Appl Environ Microbiol* **67**, 2222-2229.

Churchill, S. A., Harper, J. P. & Churchill, P. F. (1999). Isolation and characterization of a *Mycobacterium* species capable of degrading three- and four-ring aromatic and aliphatic hydrocarbons. *Appl Environ Microbiol* **65**, 549-552.

Cole, J. R., Chai, B., Farris, R. J., Wang, Q., Kulam, S. A., McGarrell, D. M., Garrity, G. M. & Tiedje, J. M. (2005). The Ribosomal Database Project (RDP-II): sequences and tools for high-throughput rRNA analysis. *Nucleic Acids Res* **1**, 294-296.

Cozzarelli, I. M., Eganhouse, R. P. & Daedecker, M. J. (1990). Transformation of monoaromatic hydrocarbons to organic acids in anoxic groundwater environment. *Environ Geol Water Sci* **16**, 135-141.

Cozzarelli, I. M., Baedecker, M. J., Eganhouse, R. P. & Goerlitz, D. F. (1994). The geochemical evolution of low-molecular-weight organic acids derived from the degradation of petroleum contaminants in groundwater. *Geochim Cosmochim Acta* **58**, 863-877.

Dell-Engineering (1992). Remedial Action Plan for Crystal Refining Company, 801 North Williams Street, Carson City, MI., Report DEI No. 921660. Holland, MI.

DeRyck, S. M., Redman, J. D. & Annan, A. P. (1993). Geophysical monitoring of a controlled kerosene spill. In *Symposium on the Application of Geophysics to Engineering and Environmental Probelms*, pp. 5-20. San Diego, CA.

Dojka, M. A., Hugenholtz, P., Haack, S. & Pace, N. (1998). Microbial diversity in a hydrocarbon- and chlorinated-solvent-contaminated aquifer undergoing intrinsic bioremediation. *Appl Environ Microbiol* **64**, 3869-3877.

Duris, J. W. (2002). Microbial community structure in hydrocarbon impacted sediment associated with anomalous geophysical signatures. In *Biological Sciences*. Kalamazoo, MI: Western Michigan University.

Feris, K. P., Hristova, K., Gebreyesus, B., Mackay, D. & Scow, K. M. (2004). A shallow BTEX and MTBE contaminated aquifer supports a diverse microbial community. *Microb Ecol* **48**, 589-600.

Finneran, K. T., Johnsen, C. V. & Lovely, D. R. (2003). *Rhodoferax ferrireducens* sp. nov., a psychrotolerant, facultatively anaerobic bacterium that oxidizes acetate with the reduction of Fe(III). *Int J Sys Evol Microbiol* **53**, 669-673.

Fuerst, J. (2004). Planctomycetes: A phylum of emerging interest for microbial evolution and ecology. *World Federation for Culture Collections Newsletter* **38**, 1-11.

Geddie, J. L. & Sutherland, I. W. (1993). Uptake of metals by bacterial polysaccharides. *J Appl Bacteriol* **74**, 467-472.

Haack, S. K. & Bekins, B. A. (2000). Microbial populations in contaminant plumes. *Hydrogeol J* **8**, 63-76.

Hayes, L. A. & Lovely, D. R. (2002). Specific 16S rDNA sequences associated with naphthalene degradation under sulfate-reducing conditions in harbor sediments. *Microbial Ecology* **43**, 134-145.

Hersman, L., Maurice, P. & Sposito, G. (1996). Iron acquisition from hydrous Fe(III)-oxides by an aerobic *Pseudomonas* sp. . *Chem Geol* **132**, 25-31.

Heyrman, J., Vanparys, B., Logan, N. A., Balcaen, A., Rodriquez-Diaz, M., Felske, A. & De Vos, P. (2004). *Bacillus novalis* sp. nov., *Bacillus vireti* sp. nov., *Bacillus soli* sp. nov., *Bacillus bataviensis* sp. nov., and *Bacillus drentensis* sp. nov., from the Drentse A grasslands. *Int J Syst Evo Microbiol* **54**.

Jackson, B. E., Bhupathiraju, V. K., Tanner, R. S., Woese, C. R. & McInerney, M. J. (1999). *Syntrophus aciditrophicus* sp. nov., a new anaerobic bacterium that degrades fatty acids and benzoate in syntrophic association with hydrogen-using microorganisms. *Arch Microbiol* **171**, 107-114.

Janssen, P. (2006). Identifying the dominant soil bacterial taxa in libraries of 16S rRNA and 16S rRNA genes. *Appl Environ Microbiol* **72**, 1719-1728.

Kaplan, C. W. & Kitts, C. L. (2004). Bacterial succession in a petroleum land treatment unit. *Applied and Environmental Microbiology* **70**, 1777-1786.

Kim, D., Kim, Y., Kim, S., Kim, S. W., Zylstra, G. J., Kim, Y. M. & Kim, E. (2002). Monocyclic Aromatic Hydrocarbon Degradation by *Rhodococcus* sp. Strain DK17 *Appl Environ Microbiol* **68**, 3270-3278.

Klee, A. J. (1993). A computer program for the determination of most probable number and its confidence limits. *J Microbiol Methods* **18**, 91-98.

Leadbetter, J. R., T.M., S., Graber, J. R. & Breznak, J. A. (1999). Acetogenesis from H_2 plus CO_2 by Spirochetes from termite guts. *Science* **283**, 686-689.

Lee, J. Y., Cheon, J. Y., Lee, K. K., Lee, S. Y. & Lee, M. H. (2001). Factors affecting the distribution of hydrocarbon contaminants and hydrogeochemical parameters in a shallow sand aquifer. *J Cont Hydrol* **50**, 139-158.

Lies, D. P., Hernandez, M. E., Kappler, A., Mielke, R. E., Gralnick, J. A. & Newman, D. K. (2005). *Shewanella oneidensis* MR-1 uses overlapping pathways for iron reduction at a distance and by direct contact under conditions relevant for biofilms. *Applied and Environmental Microbiology* **71**, 4414-4426.

Macnaughton, S. J., Stephen, J. R., Venosa, A. D., Davis, G. A., Chang, Y. & White, D. C. (1999). Microbial population changes during bioremediation of an experimental oil spill. *Appl Environ Microbiol* **65**, 3566-3574.

Madigan, M. T., Martinko, J. M. & Parker, J. (2003). *Brock biology of microorganisms, 10th ed.* Upper Saddle River, NJ: Pearson Education.

Margesin, R. & Schinner, F. (2001). Bioremediation (natural attenuation and biostimulation) of diesel-oil-contaminated soil in an alpine glacier skiing area. *Appl Environ Microbiol* **67**, 3127-3133.

McMahon, P. B., Vroblesky, D. A., Bradley, P. M., Chapelle, F. H. & Gullett, C. D. (1995). Evidence for enhanced mineral dissolution in organic acid-rich shallow ground water. *Ground Water* **33**, 207-216.

Newman, D. K. & Banfield, J. F. (2002). Geomicrobiology: How molecular-scale interactions underpin biogeochemical systems. *Environmental Microbiology* **296**, 1071-1077.

Ntarlagiannis, D., Williams, K. H., Slater, L. & Hubbard, S. (2005). On the low frequency electrical response to microbially induced sulfide precipitation. *J Geophys Res* **110**, G02009, doi:02010.01029/02005JG000024. .

Pace, N. R. (1997). A molecular view of microbial diversity and the biosphere. *Science* **276**, 734-740.

Ranjard, L., Poly, F., Combrisson, J., Richaume, A., Gourbiere, F., Thioulouse, J. & Nazaret, S. (2000). Heterogeneous cell density and genetic structure of bacterial pools assoiated with various soil microenvironments as determined by enumeration and DNA fingerprinting approach (RISA). *Microb Ecol* **39**, 263-272.

Rappe, M. S. & Giovannoni, S. J. (2003). The uncultured microbial majority. *Annu Rev Microbiol* **57**, 369-394.

Reguera, G., McCarthy, K. D., Mehta, T., Nicoll, J. S., Tuominen, M. T. & Lovely, D. R. (2005). Extracellular electron transfer via microbial nanowires. *Nature* **435**, 1098-1101.

Roberts, J. A., Hughes, B. T. & Fowle, D. A. (2004). Micro-scale mineralogic controls on microbial attachment to silicate surfaces: iron and phosphate mineral inclusions. In *Water-Rock Interaction Proceedings of the Eleventh International Symposium on Water-Rock Interaction WRI-11*, pp. 1149-1153. Edited by R. B. Wanty & R. R. Seal. Saratoga Springs, NY, USA.

Robertson, W. J., Bowman, J. P., Franzmann, P. D. & Mee, B. J. (2001). *Desulfosporosinus meridiei* sp. nov., a spore-forming sulfate-reducing bacterium isolated from gasolene-contaminated ground water. *International Journal of Systematic and Evolutionary Microbiology* **51**, 133-140.

Roling, W. F. M., Milner, M. G., Jones, D. M., Fratepietro, F., Swannell, R. P. J., Daniel, F. & Head, I. M. (2004). Bacterial community dynamics and hydrocarbon

degradation during a field-scale evaluation of bioremediation on a mudflat beach contaminated with buried oil. *Appl Environ Microbiol* **70**, 2603-2613.

Sauck, W. A. (2000). A model for the resistivity structure of LNAPL plumes and their environs in sandy sediments. *J Appl Geophys* **44**, 151-165.

Schink, B. (1997). Energetics of syntrophic cooperation in methanogenic degradation. *Microbiol Mol Biol Rev* **61**, 262-280.

Schmidt, T. M., Arieli, B., Cohen, Y., Padan, E. & Strohl, W. R. (1987). Sulfur metabolism in *Beggiatoa alba*. *J Bacteriol* **169**, 5466-5472.

Sherrod, L. A., Werkema, D.D., Sauck, W.A., Atekwana, E.A., Rossbach, S., and Atekwana, E.A. (2003). Column experiments and anomalous conductivity in hydrocarbon-impacted sands. *Eighth International Congress of the Brazilian Geophysical Society*.

Singleton, D. R., Furlong, M. A., Rathbun, S. L. & Whitman, W. B. (2001). Quantitative comparisons of 16S rRNA gene sequence libraries from environmental samples. *Appl Environ Microbiol* **67**, 4374-4376.

Soucaille, P. & Goma, G. (1986). Acetobutylic fermentation by Clostridium acetobutylicum ATCC 824: Autobacteriocin production, properties, and effects. *Curr Microbiol* **13**, 163-169.

Telford, W. M., Geldart, L. P. & Sheriff, R. E. (1990). *Applied Geophysics* 2nd edn. Cambridge, UK: Cambridge University Press.

Thompson, J. D., Gibson, T. J., Plewniak, F., Jeanmougin, F. & Higgins, D. G. (1997). The ClustalX windows interface: flexible strategies for multiple sequence alignment aided by quality analysis tools. *Nucleic Acids Res* **24**, 4876-4882.

Tulis, D. S. (1997). Issues associated with natural attenuation. Washington, D.C.: U.S. Environmental Protection Agency, Washington, D.C.

U.S.EPA (2006). Cleaning up underground storage tank system releases.

Van Hamme, J. D., Singh, A. & Ward, O. P. (2003). Recent Advances in Petroleum Microbiology. *Microbiol Mol Biol Rev* **67**, 503–549.

Venosa, A. D., Suidan, M. T., Wrenn, B. A., Strohmeier, K. L., Haines, J. R., Eberhart, B. L., King, D. & Holder, E. (1996). Bioremediation of an experimental oil spill on the shoreline of Delaware bay. *Environ Sci Technol* **30**, 1764-1775.

Walworth, J. L. & Reynolds, C. M. (1995). Bioremediation of a petroleum-contaminated cryic soil: Effects of phosphorous, nitrogen, and temperature. *J Soil Contam* **4**, 299-310.

Werkema, D. D. (2002). Geoelectrical response of an aged LNAPL plume: Implications for monitoring natural attenuation. In *Geosciences Department.* Kalamazoo, MI, USA: Western Michigan University.

Whiteley, A. S. & Bailey, M. J. (2000). Bacterial community structure and physiological state within an industrial phenol bioremediation system. *Appl Environ Microbiol* **66**, 2400-2407.

Williams, K. H., Ntarlagiannis, D., Slater, L., Dohnalkova, A., Hubbard, S. S. & Banfield, J. F. (2005). Geophysical imaging of stimulated microbial biomineralization. *Environ Sci Tech* **39**, 7592-7600.

Wrenn, B. A. & Venosa, A. D. (1996). Selective enumeration of aromatic and aliphatic hydrocarbon degrading bacteria by a most-probable-number procedure. *Can J Microbiol* **42**, 252-258.

Wu, J. H., Liu, W. T., Tseng, I. C. & Cheng, S. S. (2001). Characterization of microbial consortia in a terephthalate-degrading anaerobic granular sludge system. *Microbiology* **147**, 373-382.

Zhou, J., Xia, B., Huang, H., Palumbo, A. V. & Tiedje, J. M. (2004). Microbial diversity and heterogeneity in sandy subsurface soils. *Appl Environ Microbiol* **70**, 1723-1734.

Zita, A. & Hemansoon, M. (1994). Effects of ionic strength on bacterial adhesion and stability of flocs in wastewater activated sludge system. *Appl Environ Microbiol* **60**, 3041-3048.